



“Features of Topology in Condensed Matter Physics”

Prof. Andrés Camilo García Castro, Ph.D.

Escuela de Física, Universidad Industrial de Santander,

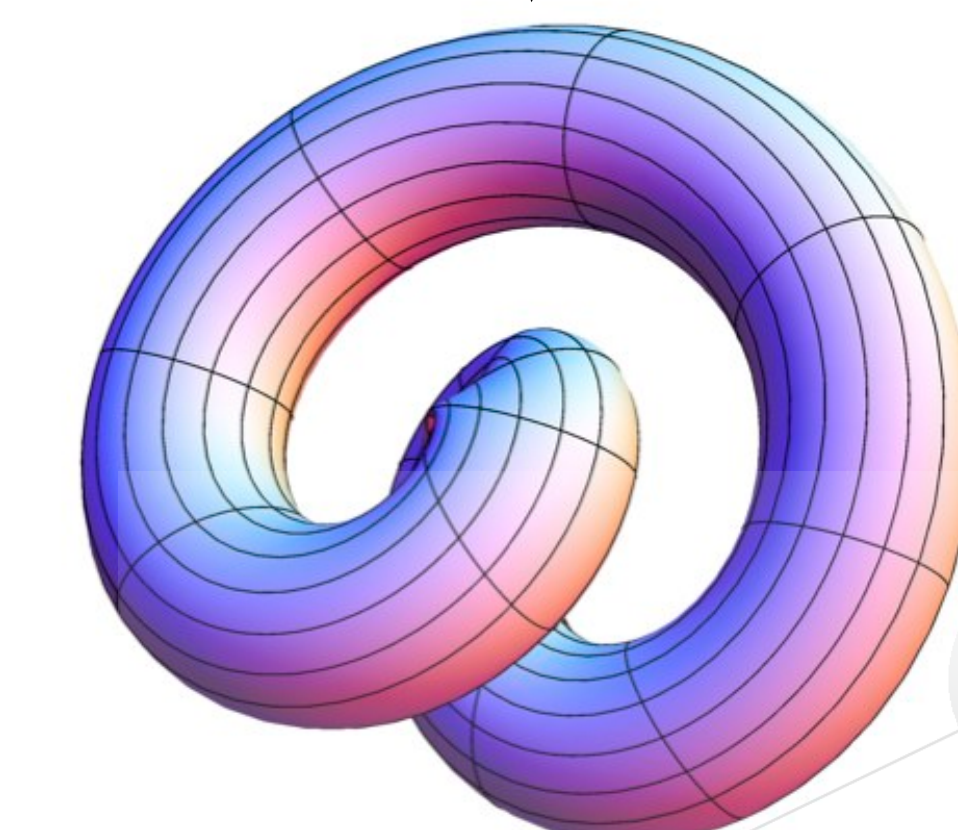
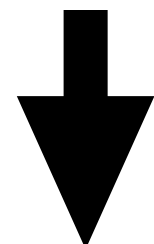
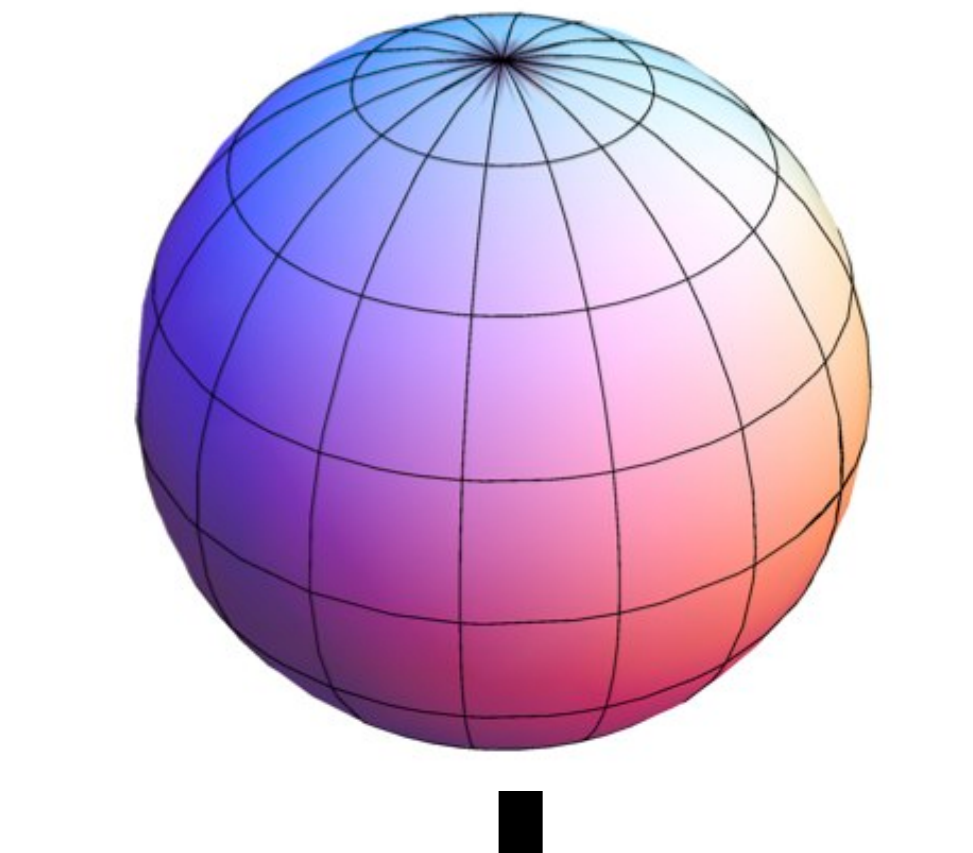
Bucaramanga - Santander (Colombia).

email: acgarcia@uis.edu.co

Universidad
Industrial de
Santander



- ✓ Introduction: Topological effects on matter.
- ✓ Theoretical approach:
 - ✓ Linear response.
 - ✓ Berry phase, Berry connection, and Berry curvature.
 - ✓ “Berry” effects in condensed matter.
- ✓ Ferroelectric Polarization.
- ✓ Orbital magnetization.
- ✓ Topological materials: Insulators, metals, semiconductors.
- ✓ Theoretical-computational approach: Wannier Functions.
- ✓ TB-models within the WF representation.
 - ✓ Graphene Model.
- ✓ What's next...?





REVIEWS OF MODERN PHYSICS, VOLUME 82, JULY–SEPTEMBER 2010

Berry phase effects on electronic properties

Di Xiao

Materials Science and Technology Division, Oak Ridge National Laboratory, Oak Ridge, Tennessee 37831, USA

Ming-Che Chang

Department of Physics, National Taiwan Normal University, Taipei 11677, Taiwan

Qian Niu

Department of Physics, The University of Texas at Austin, Austin, Texas 78712, USA

(Published 6 July 2010)

Ever since its discovery the notion of Berry phase has permeated through all branches of physics. Over the past three decades it was gradually realized that the Berry phase of the electronic wave function can have a profound effect on material properties and is responsible for a spectrum of phenomena, such as polarization, orbital magnetism, various (quantum, anomalous, or spin) Hall effects, and quantum charge pumping. This progress is summarized in a pedagogical manner in this review. A brief summary of necessary background is given and a detailed discussion of the Berry phase effect in a variety of solid-state applications. A common thread of the review is the semiclassical formulation of electron dynamics, which is a versatile tool in the study of electron dynamics in the presence of electromagnetic fields and more general perturbations. Finally, a requantization method is demonstrated that converts a semiclassical theory to an effective quantum theory. It is clear that the Berry phase should be added as an essential ingredient to our understanding of basic material properties.

DOI: [10.1103/RevModPhys.82.1959](https://doi.org/10.1103/RevModPhys.82.1959)

PACS number(s): 71.70.Ej, 72.10.Bg, 73.43.-f, 77.84.-s



REVIEWS OF MODERN PHYSICS, VOLUME 81, JANUARY–MARCH 2009

The electronic properties of graphene

A. H. Castro Neto

Department of Physics, Boston University, 590 Commonwealth Avenue, Boston, Massachusetts 02215, USA

F. Guinea

Instituto de Ciencia de Materiales de Madrid, CSIC, Cantoblanco, E-28049 Madrid, Spain

N. M. R. Peres

Center of Physics and Department of Physics, Universidade do Minho, P-4710-057, Braga, Portugal

K. S. Novoselov and A. K. Geim

Department of Physics and Astronomy, University of Manchester, Manchester, M13 9PL, United Kingdom

(Published 14 January 2009)

This article reviews the basic theoretical aspects of graphene, a one-atom-thick allotrope of carbon, with unusual two-dimensional Dirac-like electronic excitations. The Dirac electrons can be controlled by application of external electric and magnetic fields, or by altering sample geometry and/or topology. The Dirac electrons behave in unusual ways in tunneling, confinement, and the integer quantum Hall effect. The electronic properties of graphene stacks are discussed and vary with stacking order and number of layers. Edge (surface) states in graphene depend on the edge termination (zigzag or armchair) and affect the physical properties of nanoribbons. Different types of disorder modify the Dirac equation leading to unusual spectroscopic and transport properties. The effects of electron-electron and electron-phonon interactions in single layer and multilayer graphene are also presented.

DOI: [10.1103/RevModPhys.81.109](https://doi.org/10.1103/RevModPhys.81.109)

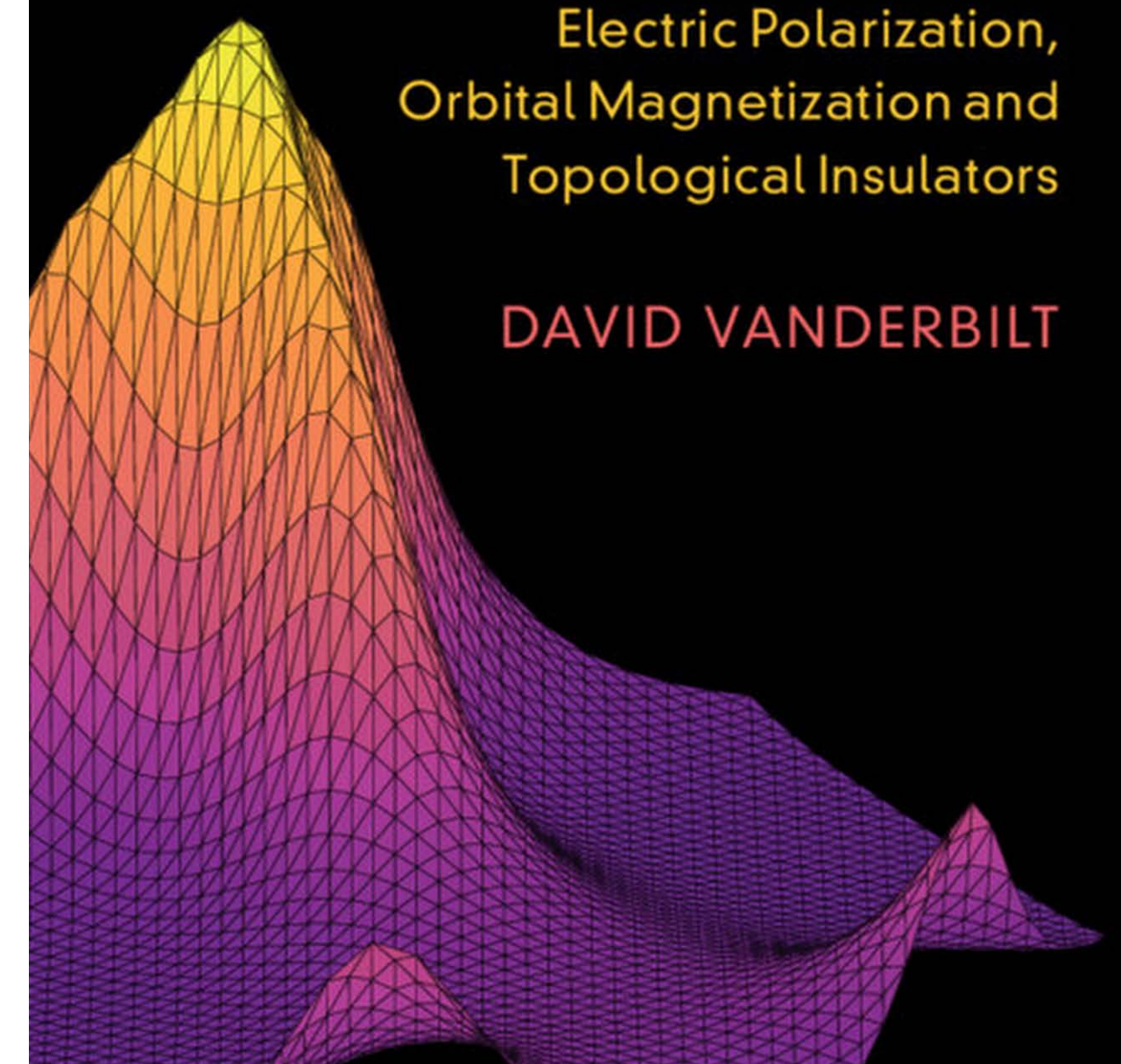
PACS number(s): 81.05.Uw, 73.20.-r, 03.65.Pm, 82.45.Mp



Berry Phases in Electronic Structure Theory

Electric Polarization,
Orbital Magnetization and
Topological Insulators

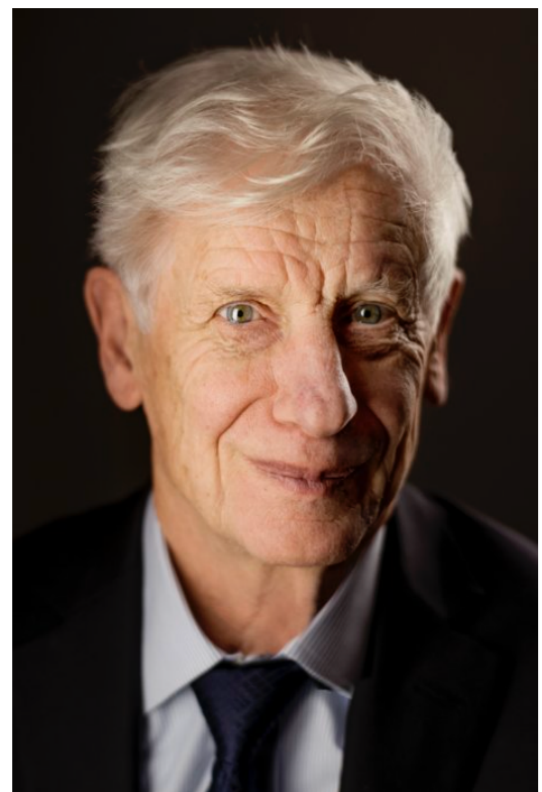
DAVID VANDERBILT



The Nobel Prize in Physics 2016

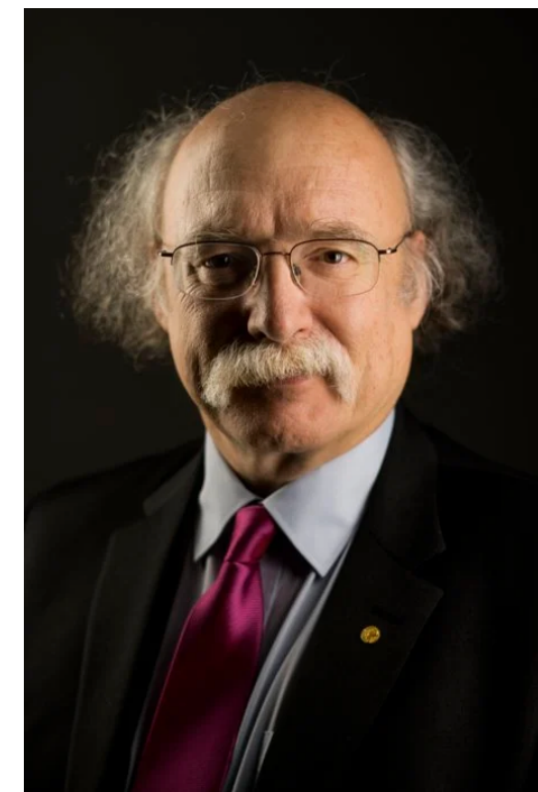
David J. Thouless
F. Duncan M. Haldane
J. Michael Kosterlitz

Share this



© Nobel Media AB. Photo: A.
Mahmoud

David J. Thouless
Prize share: 1/2



© Nobel Media AB. Photo: A.
Mahmoud

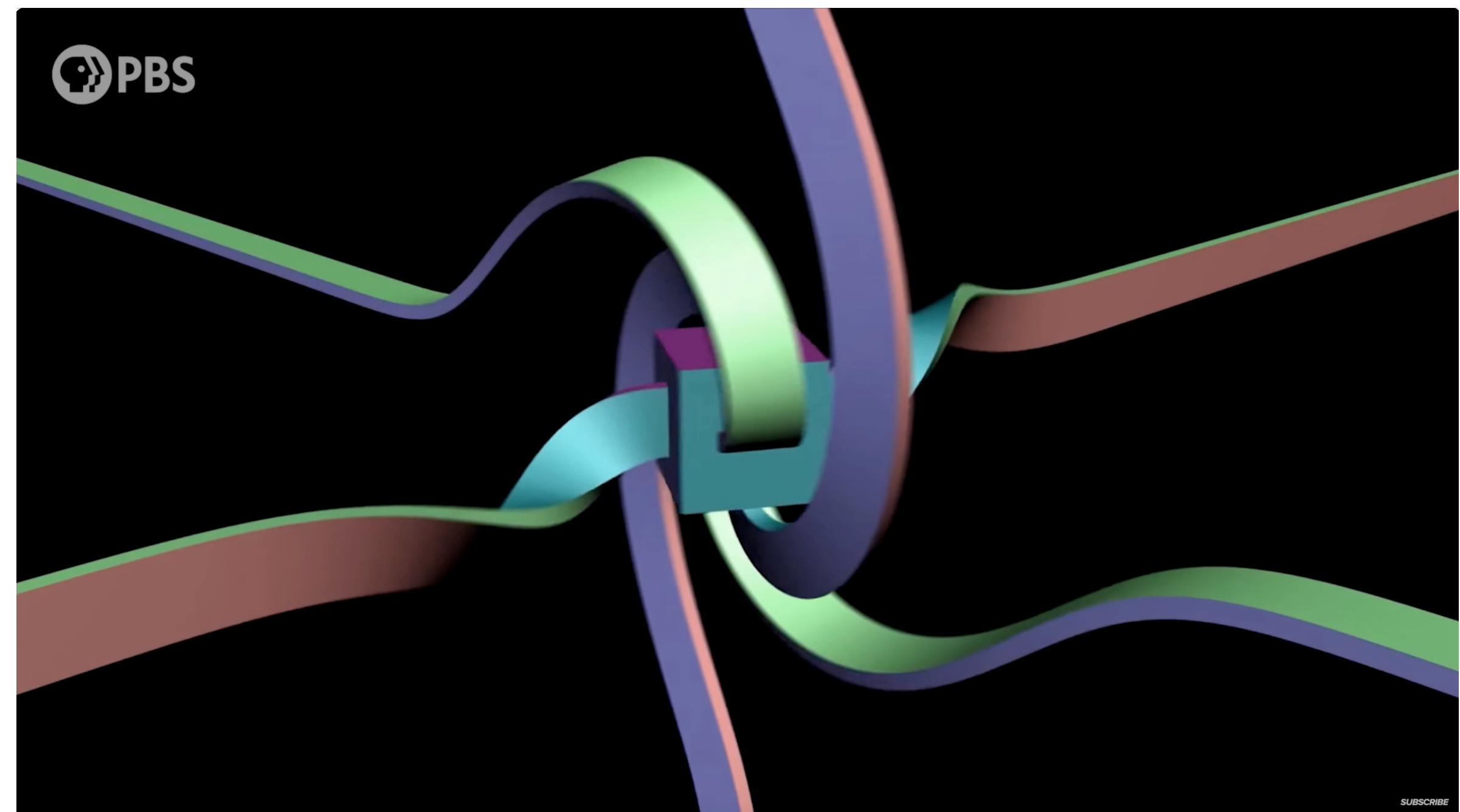
F. Duncan M. Haldane
Prize share: 1/4



© Nobel Media AB. Photo: A.
Mahmoud

J. Michael Kosterlitz
Prize share: 1/4

The Nobel Prize in Physics 2016 was awarded with one half to David J. Thouless, and the other half to F. Duncan M. Haldane and J. Michael Kosterlitz "for theoretical discoveries of topological phase transitions and topological phases of matter"



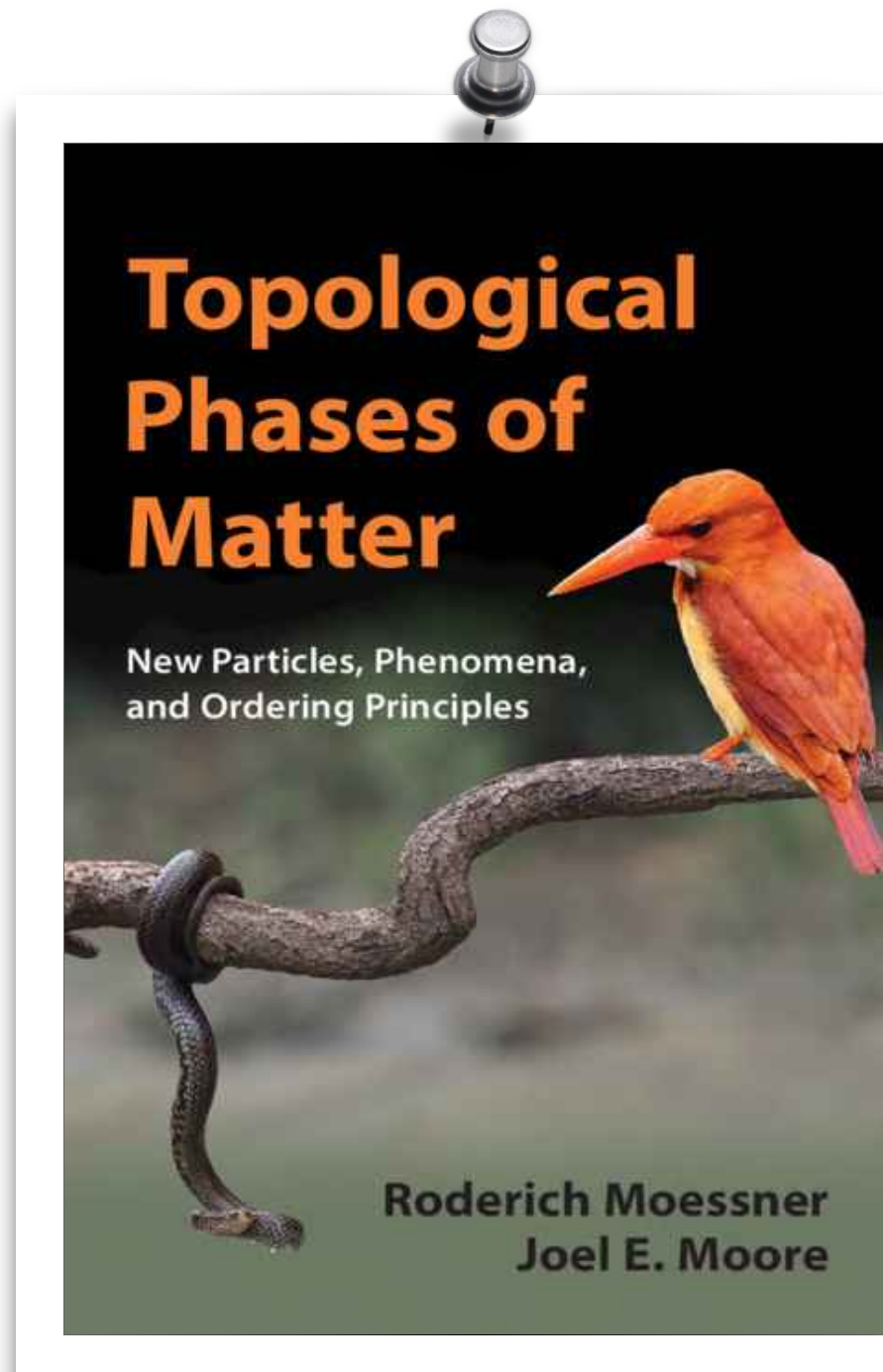
PBS Space Time (Youtube), Electrons DO NOT spin



“... in these days the angel of topology and the devil of abstract algebra fight for the soul of each individual mathematical domain...”

Hermann Weyl (1939)

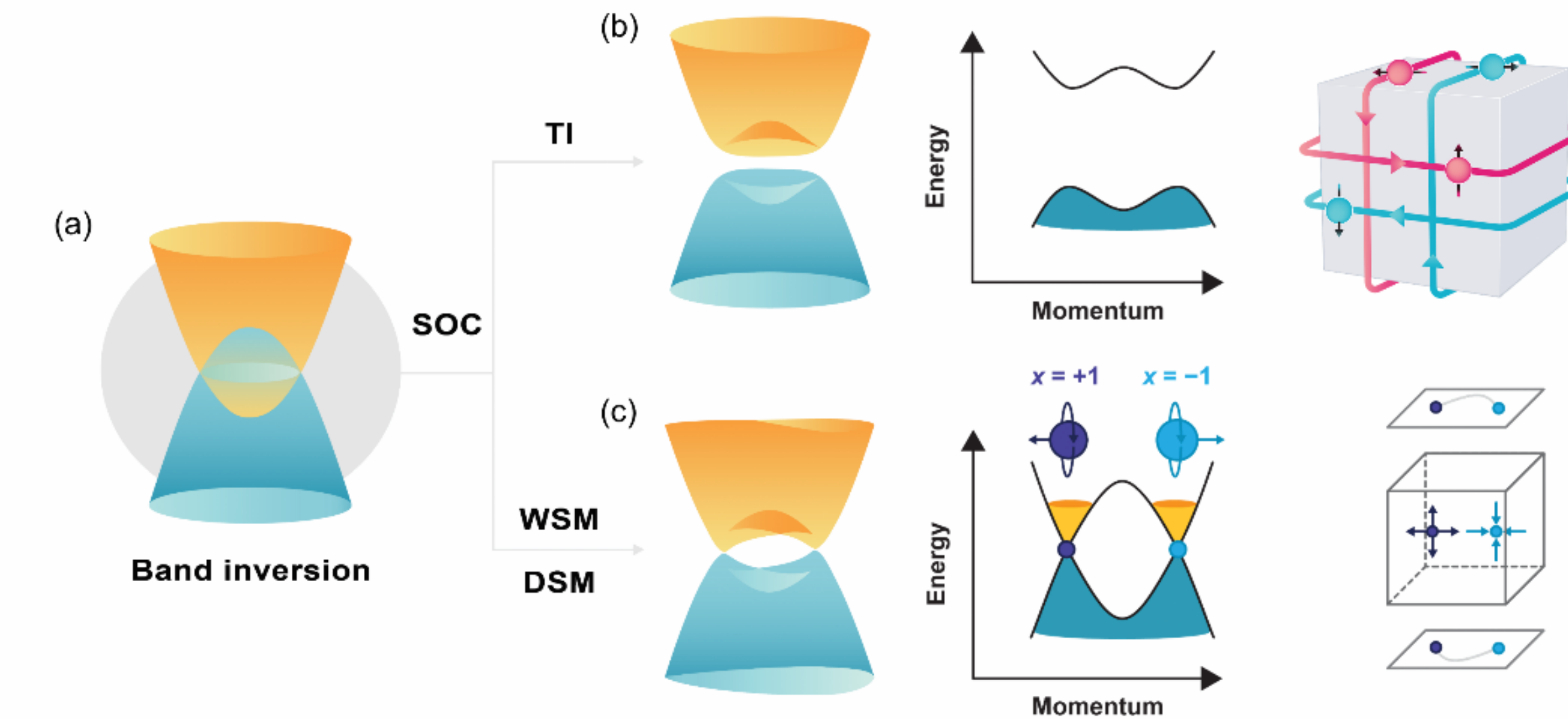
Topology studies properties of spaces that are invariant under any continuous deformation. It is sometimes called "rubber-sheet geometry" because the objects can be stretched and contracted like rubber, but cannot be broken.



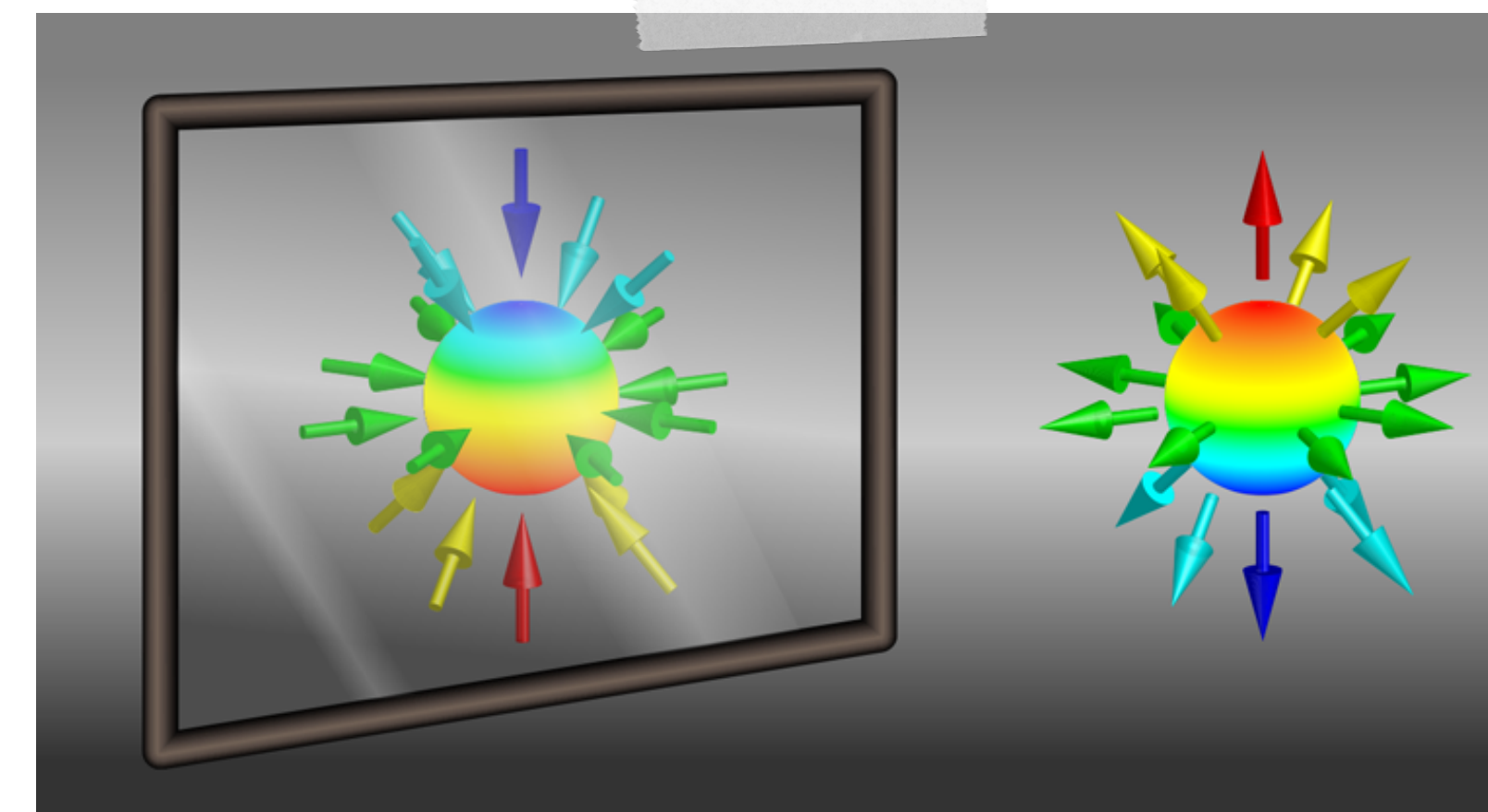
“...Condensed matter physics” is a catchall term for systems of many constituent particles in which the fundamental objects are electrons, nuclei, and photons described by electromagnetism and quantum mechanics.”

“...Condensed matter physics deals with the question of how phenomena such as crystalline order, or waves, or superconductivity, emerge from a collection of particles for which individually these concepts do not even have a meaning: no water molecule will ever form a wave, nor even a ripple, on its own.”





Claudia Feller and J. Gooth, ArXiv, [arXiv:2205.05809](https://arxiv.org/abs/2205.05809) (2022).



Existence of the “holy trinity”: Dirac, Majorana, and Weyl quasiparticles

M. Sakano et al., Phys. Rev. Lett. 124, 136404 (2020).

$$H(\lambda)|n(\lambda)\rangle = E_n(\lambda)|n(\lambda)\rangle$$



$$(E_n - H)|\partial_\lambda n\rangle = \partial_\lambda(H - E_n)|n\rangle$$



$$\partial_\lambda E_n = \langle n|(\partial_\lambda H)|n\rangle.$$



$$(E_n - H)|\partial_\lambda n\rangle = \mathcal{Q}_n (\partial_\lambda H) |n\rangle$$

Sternheimer equation,

$$\mathcal{Q}_n = \sum_{m \neq n} |m\rangle\langle m| = 1 - \mathcal{P}_n$$



$$|\partial_\lambda n\rangle = -iA_n|n\rangle + \sum_{m \neq n} \frac{|m\rangle\langle m|}{E_n - E_m} (\partial_\lambda H) |n\rangle$$

$$A_n(\lambda) = i\langle n|\partial_\lambda n\rangle$$

Berry Connection...!



$$|n(\lambda)\rangle = e^{i \int A_n(\lambda) d\lambda} |n_0\rangle.$$



$$\frac{\partial^2 E}{\partial \lambda_A \partial \lambda_B} = \frac{\partial \langle A \rangle}{\partial \lambda_B} = \frac{\partial \langle B \rangle}{\partial \lambda_A} = \sum_n^{\text{occ}} 2\text{Re} \langle n|AT_nB|n\rangle$$

A Berry phase is a phase angle (i.e., running between 0 and 2π) that describes the global phase evolution of a complex vector as it is carried around a path in its vector space.

$$\phi = -\text{Im} \ln [\langle u_0 | u_1 \rangle \langle u_1 | u_2 \rangle \dots \langle u_{N-1} | u_0 \rangle]$$

$$|u_a\rangle = |u_d\rangle = \frac{1}{\sqrt{2}} \begin{pmatrix} 1 \\ 1 \end{pmatrix}, \quad |u_b\rangle = \frac{1}{\sqrt{2}} \begin{pmatrix} 1 \\ e^{2\pi i/3} \end{pmatrix}, \quad |u_c\rangle = \frac{1}{\sqrt{2}} \begin{pmatrix} 1 \\ e^{4\pi i/3} \end{pmatrix}$$

$$\phi = -\text{Im} \ln [\langle u_a | u_b \rangle \langle u_b | u_c \rangle \langle u_c | u_a \rangle] = -\text{Im} \ln \left[\left(\frac{e^{\pi i/3}}{2} \right)^3 \right] = -\pi$$

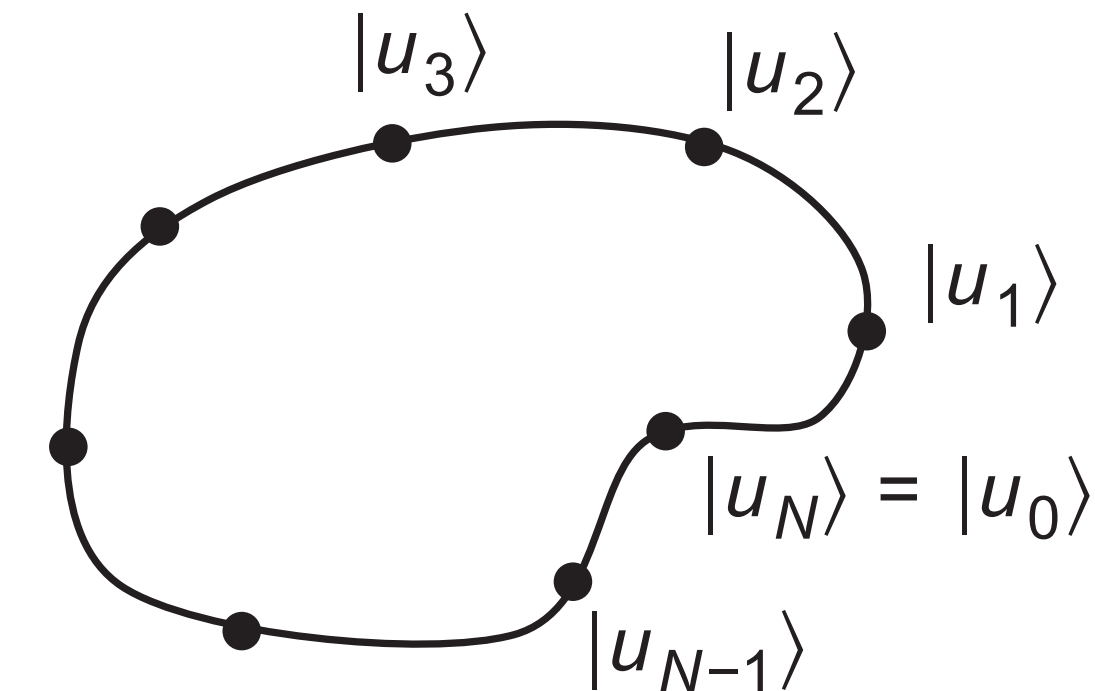


Figure 3.1 Illustration of the evolution of some complex unit vector $|u\rangle$ around a path in parameter space. The first and last points $|u_0\rangle$ and $|u_N\rangle$ are identical.

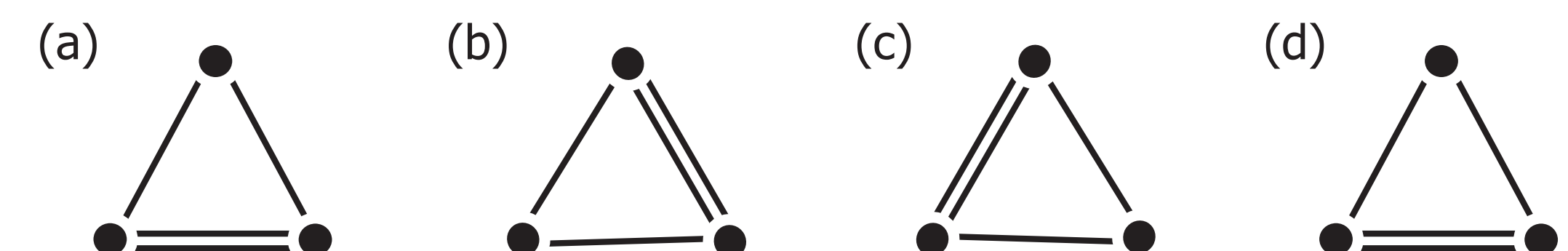


Figure 3.2 Triangular molecule going through a sequence of distortions in which first the bottom bond, then the upper-right bond, and then the upper-left bond is the shortest and strongest of the three. The configurations in (a) and (d), representing the beginning and end of the loop, are identical.

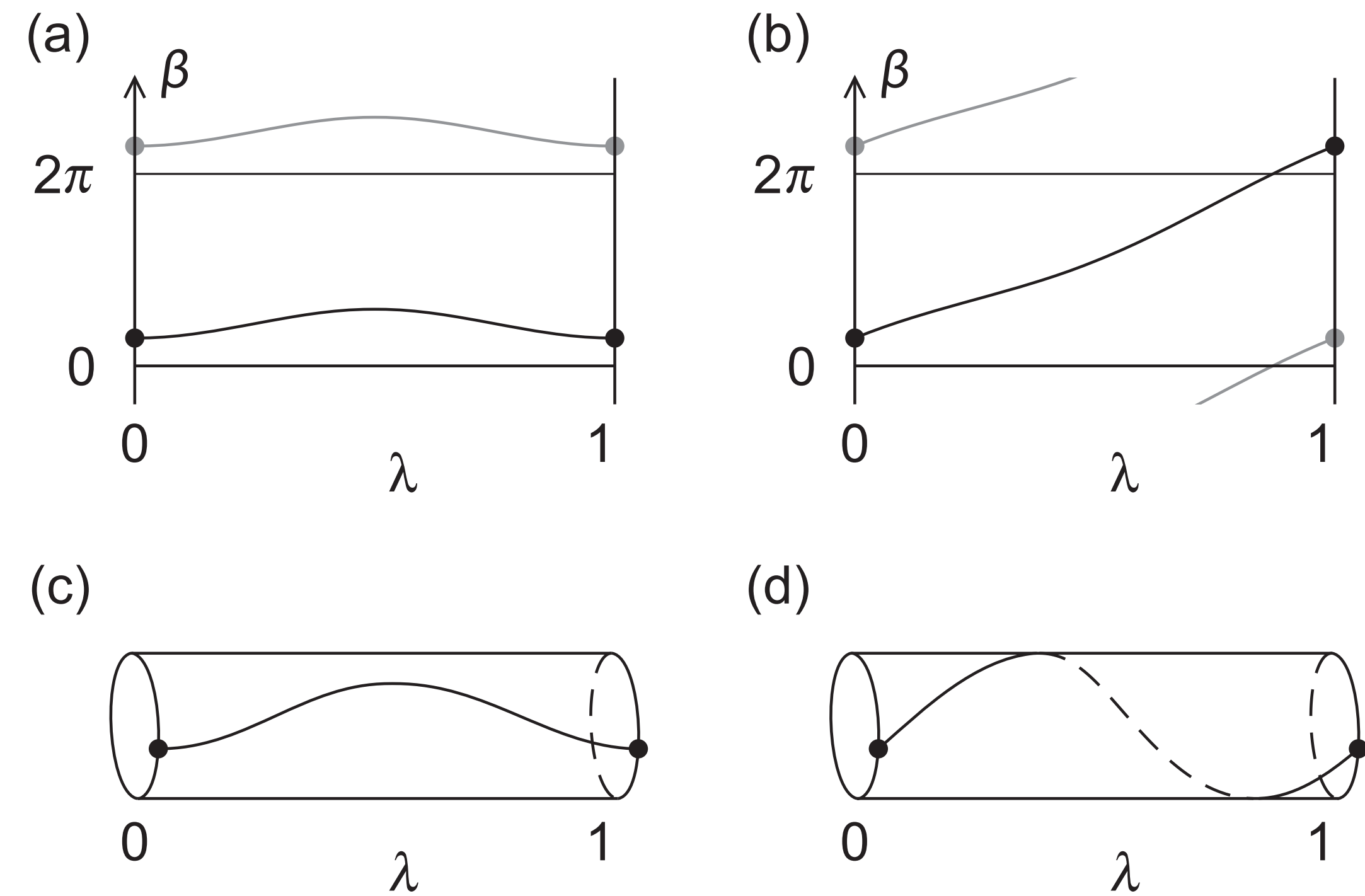


Figure 3.5 Possible behaviors of the function $\beta(\lambda)$ defining a gauge transformation through Eq. (3.15). (a–b) Conventional plots of “progressive” (a) and “radical” (b) gauge transformations, for which β returns to itself or is shifted by a multiple of 2π at the end of the loop, respectively. Gray lines show 2π -shifted periodic images. (c–d) Same as (a–b) but plotted on the surface of a cylinder to emphasize the nontrivial winding of the radical gauge transformation in (b) and (d).

$$\begin{aligned}\ln \langle u_\lambda | u_{\lambda+d\lambda} \rangle &= \ln \langle u_\lambda | \left(|u_\lambda\rangle + d\lambda \frac{d|u_\lambda\rangle}{d\lambda} + \dots \right) \\ &= \ln(1 + d\lambda \langle u_\lambda | \partial_\lambda u_\lambda \rangle + \dots) \\ &= d\lambda \langle u_\lambda | \partial_\lambda u_\lambda \rangle + \dots\end{aligned}$$

$$\phi = \oint \langle u_\lambda | i \partial_\lambda u_\lambda \rangle d\lambda$$

Berry Phase...!

$$\phi = \oint A(\lambda) d\lambda$$

$$\Omega_{\mu\nu} = \partial_\mu A_\nu - \partial_\nu A_\mu = -2 \operatorname{Im} \langle \partial_\mu u | \partial_\nu u \rangle$$

Berry Curvature...!

$$\oint_S \boldsymbol{\Omega} \cdot d\mathbf{S} = 2\pi C$$

Chern Number...!

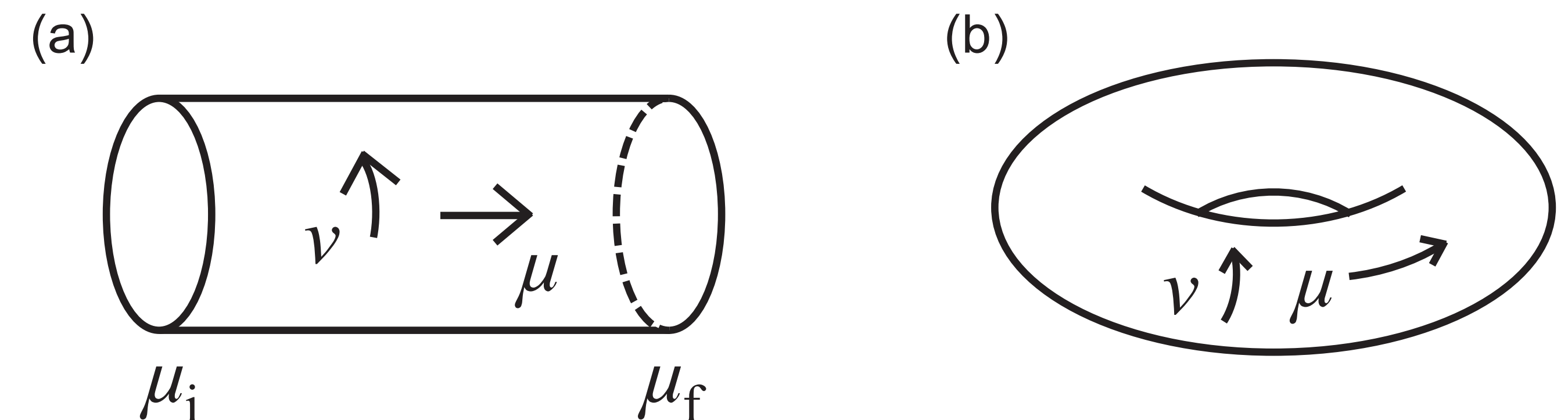


Figure 3.10 (a) Two-dimensional parameter space that is cyclic in ν (with $\nu=0$ and $\nu=1$ identified) while extending from $\mu=\mu_i$ to $\mu=\mu_f$. The topology is that of a cylinder. (b) Now μ is also cyclic, such that the topology is that of a torus.

$$\int_{-\infty}^{\infty} \psi_{nk}^*(x) \psi_{n,k+b}(x) dx = \int_{-\infty}^{\infty} e^{ibx} u_{nk}^*(x) u_{n,k+b}(x) dx$$

$$\langle u_{nk} | u_{n,k+b} \rangle = \int_0^a u_{nk}^*(x) u_{n,k+b}(x) dx$$

$$\phi_n = \oint \mathbf{A}_n(\mathbf{k}) \cdot d\mathbf{k}$$

$$C_n = \frac{1}{2\pi} \int_{\text{BZ}} \Omega_{n,xy} d^2k.$$

$$\phi_n = \oint_{\text{BZ}} A_n(k) dk = \oint_{\text{BZ}} \langle u_{nk} | i\partial_k u_{nk} \rangle$$

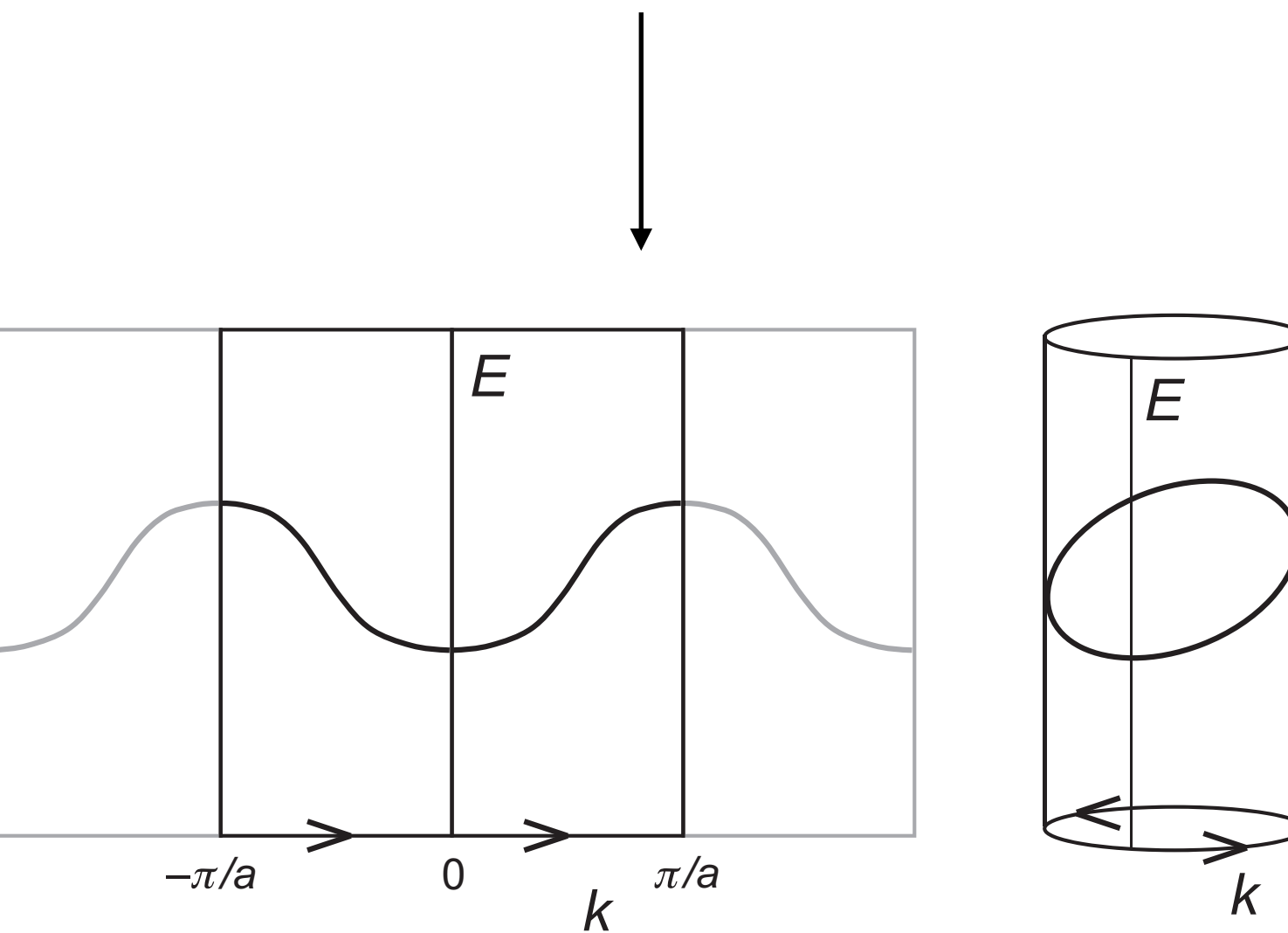


Figure 3.12 At left, conventional view of a 1D band structure, with the first BZ highlighted in black and the extended-zone scheme shown in gray. At right, a more topologically natural view in which the BZ is wrapped onto a circle and the band structure is plotted on a cylinder.

$$|w_{n\mathbf{R}}\rangle = \frac{V_{\text{cell}}}{(2\pi)^3} \int_{\text{BZ}} e^{-i\mathbf{k}\cdot\mathbf{R}} |\psi_{n\mathbf{k}}\rangle d^3k,$$

\Updownarrow FT

$$|\psi_{n\mathbf{k}}\rangle = \sum_{\mathbf{R}} e^{i\mathbf{k}\cdot\mathbf{R}} |w_{n\mathbf{R}}\rangle.$$

Wannier Functions...!

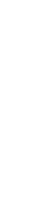
$$\langle w_{n0}| \mathbf{r} | w_{n\mathbf{R}} \rangle = \mathbf{A}_{n\mathbf{R}}.$$

$$\mathbf{A}_{n\mathbf{R}} = \frac{V_{\text{cell}}}{(2\pi)^3} \int_{\text{BZ}} e^{-i\mathbf{k}\cdot\mathbf{R}} \mathbf{A}_n(\mathbf{k}) d^3k,$$

\Updownarrow FT

$$\mathbf{A}_n(\mathbf{k}) = \sum_{\mathbf{R}} e^{i\mathbf{k}\cdot\mathbf{R}} \mathbf{A}_{n\mathbf{R}}.$$

$$\langle w_{n0} | H | w_{n\mathbf{R}} \rangle = \frac{V_{\text{cell}}}{(2\pi)^3} \int_{\text{BZ}} e^{-i\mathbf{k}\cdot\mathbf{R}} \langle u_{n\mathbf{k}} | H_{\mathbf{k}} | u_{n\mathbf{k}} \rangle d^3k,$$

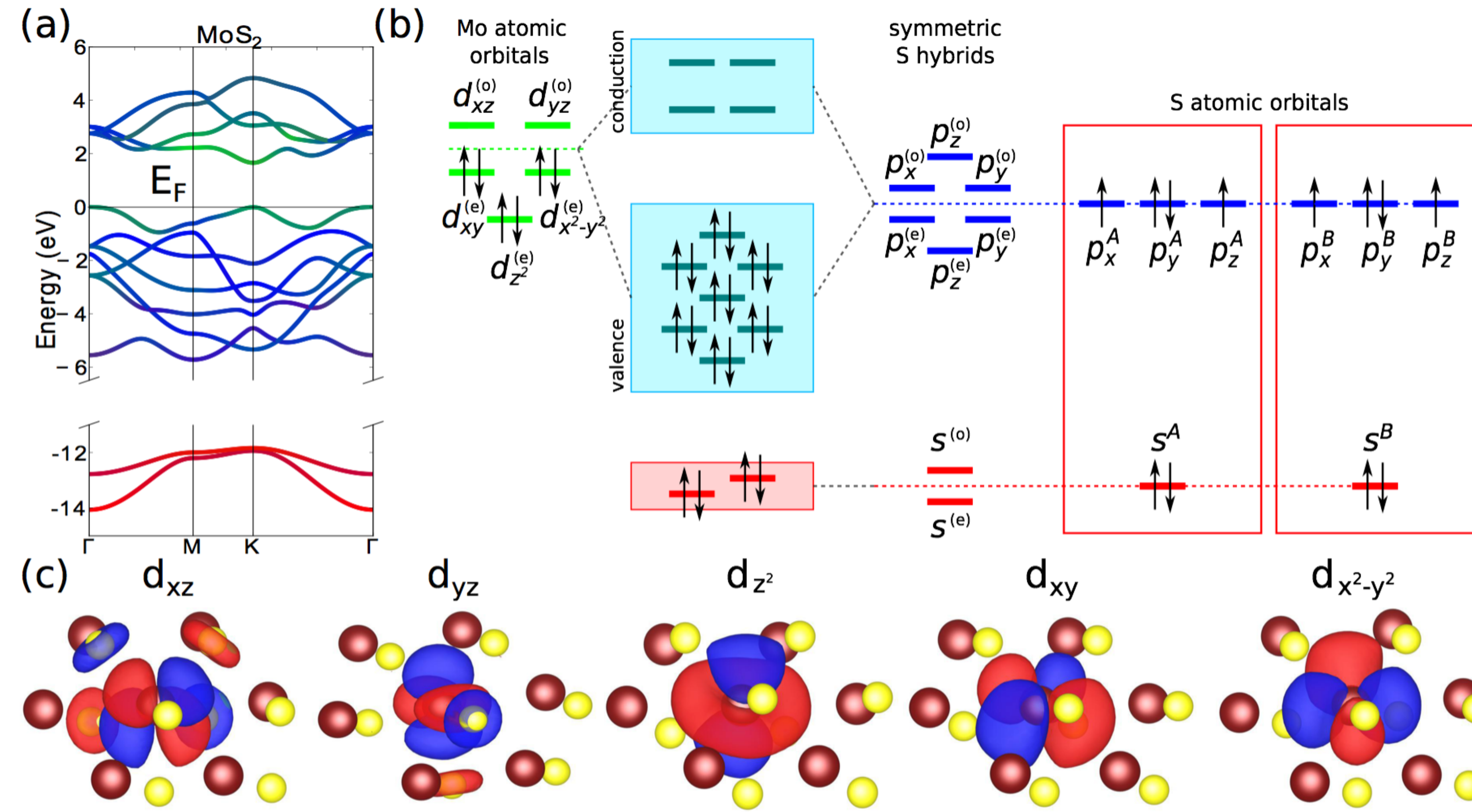


$$\bar{\mathbf{r}}_n = \frac{V_{\text{cell}}}{(2\pi)^3} \int_{\text{BZ}} \mathbf{A}_n(\mathbf{k}) d^3k$$

$$= \frac{V_{\text{cell}}}{(2\pi)^3} \int_{\text{BZ}} \langle u_{n\mathbf{k}} | i\nabla_{\mathbf{k}} u_{n\mathbf{k}} \rangle d^3k.$$



$$\bar{x}_n = a \frac{\phi_n}{2\pi}.$$

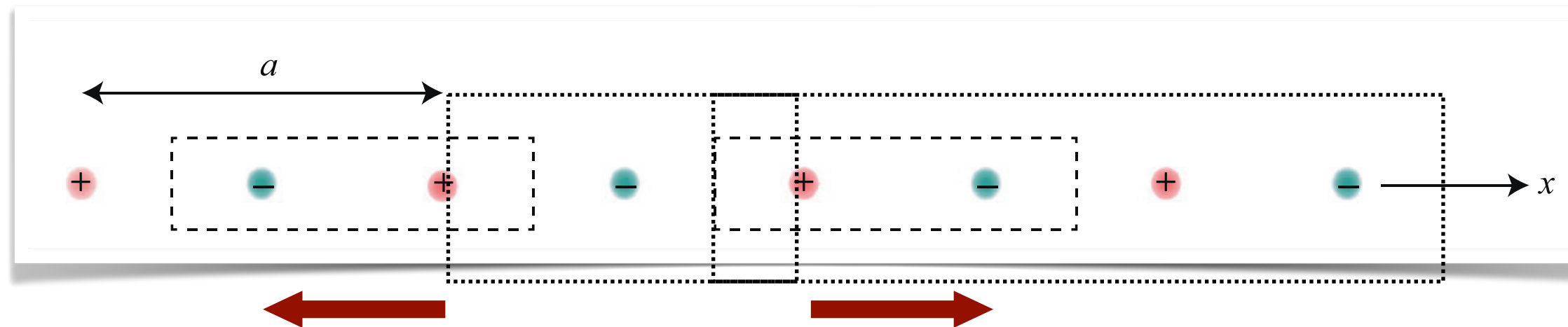


https://stevetorr.github.io/wannier_shift/overview.html

$$\mathbf{d} = \sum_i q_i \mathbf{r}_i;$$

$$\mathbf{d} = \int e n(\mathbf{r}) \mathbf{r} d\mathbf{r}.$$

How to compute such parameters in solid state physics?

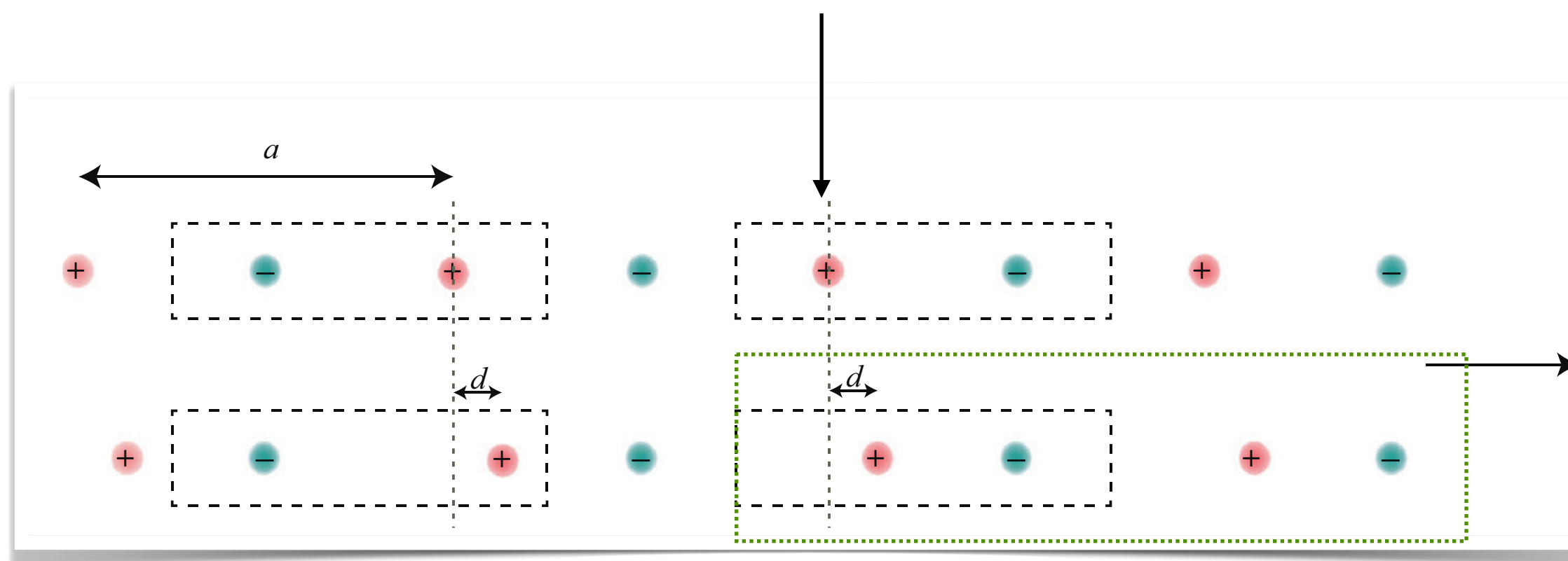


- S. Baroni, P. Giannozzi, A. Testa, Phys. Rev. Lett. 58 (1987) 1861–1864.
 R.D. King-Smith, D. Vanderbilt, Phys. Rev. B 47 (1993) R1651–R1654.
 R.D. King-Smith, D. Vanderbilt, Phys. Rev. B 49 (1994) 5828–5844.
 R. Resta, Rev. Mod. Phys. 66 (1994) 899–915.

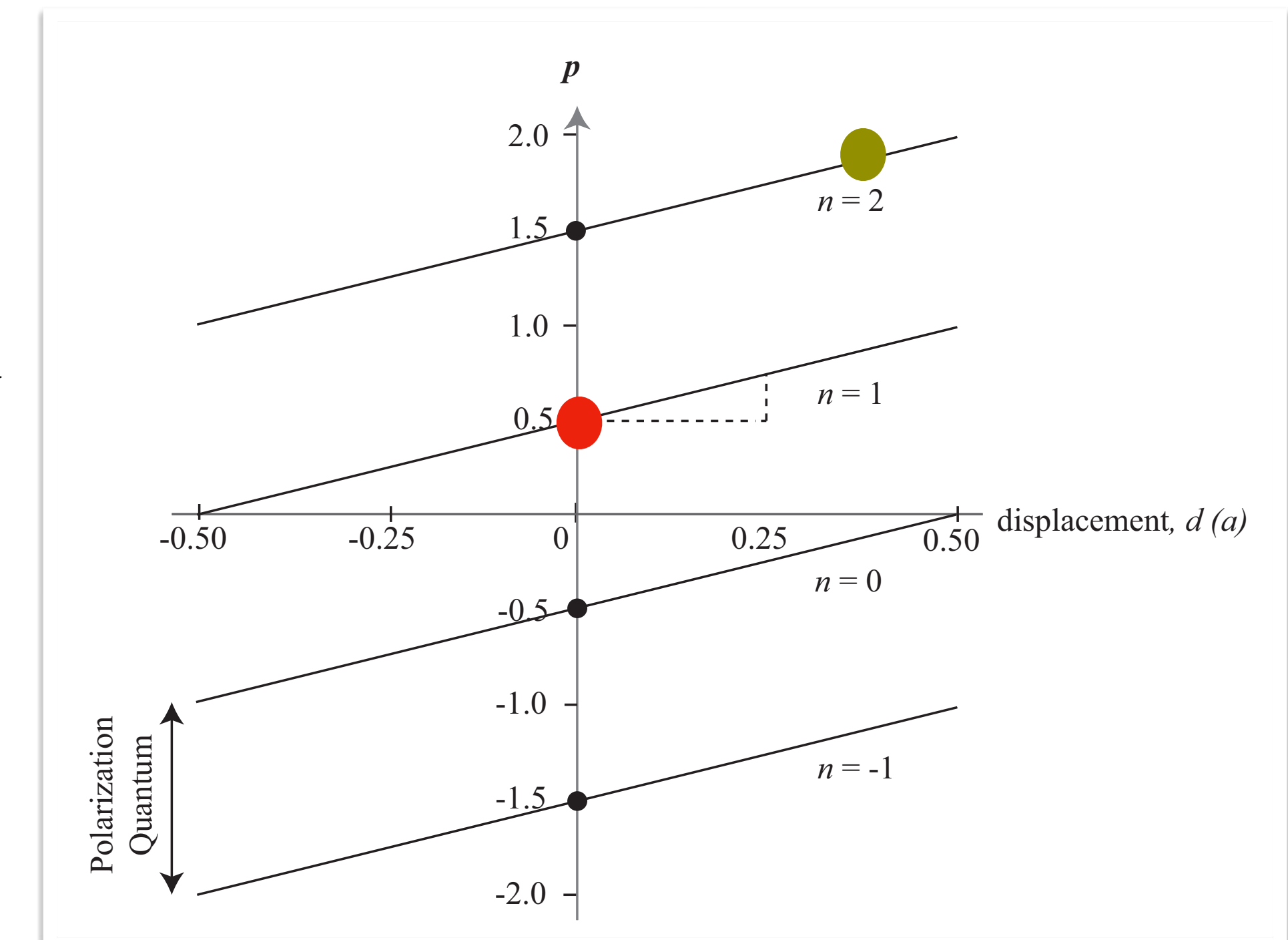
...multi-valuedness of the bulk polarization.

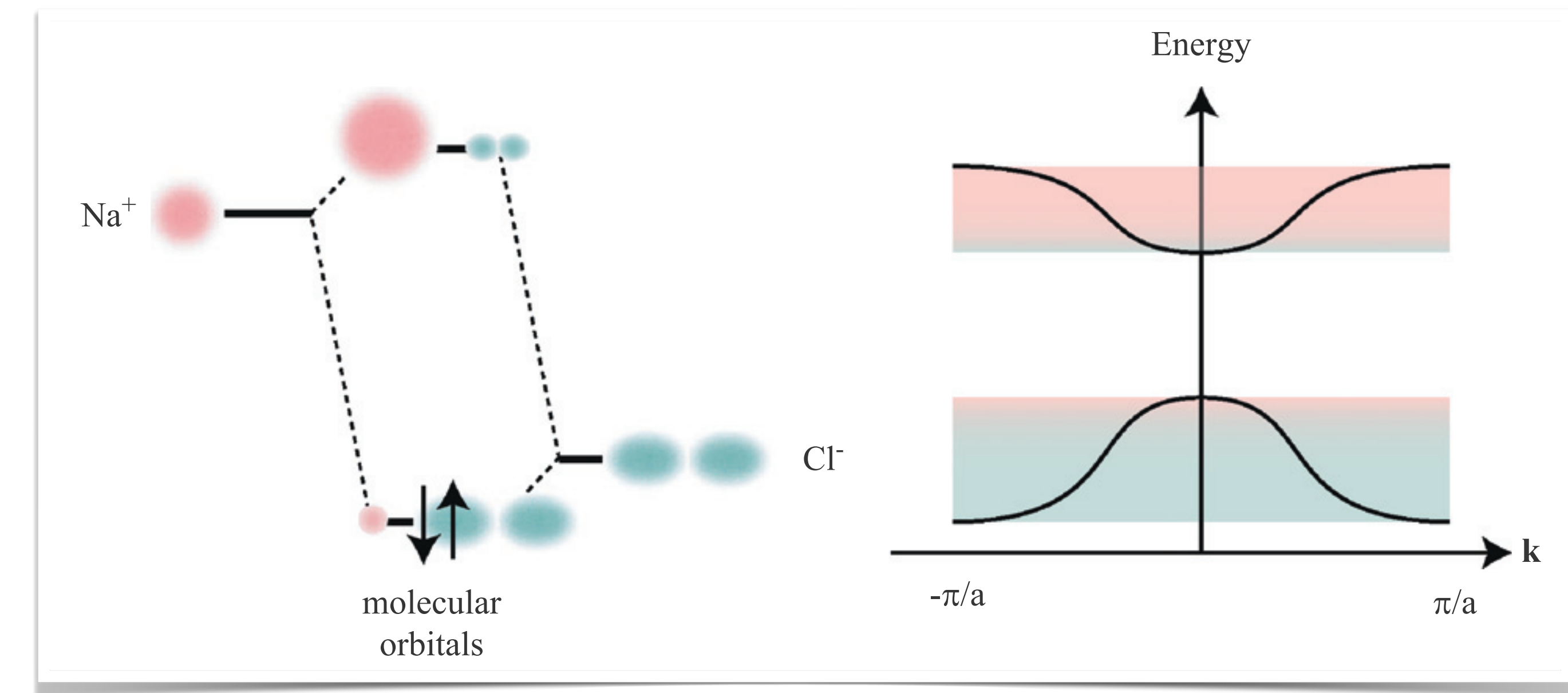
We call this collection of polarization values the polarization lattice.

In this case: $-5/2, -3/2, -1/2, +1/2, +3/2, +5/2$.

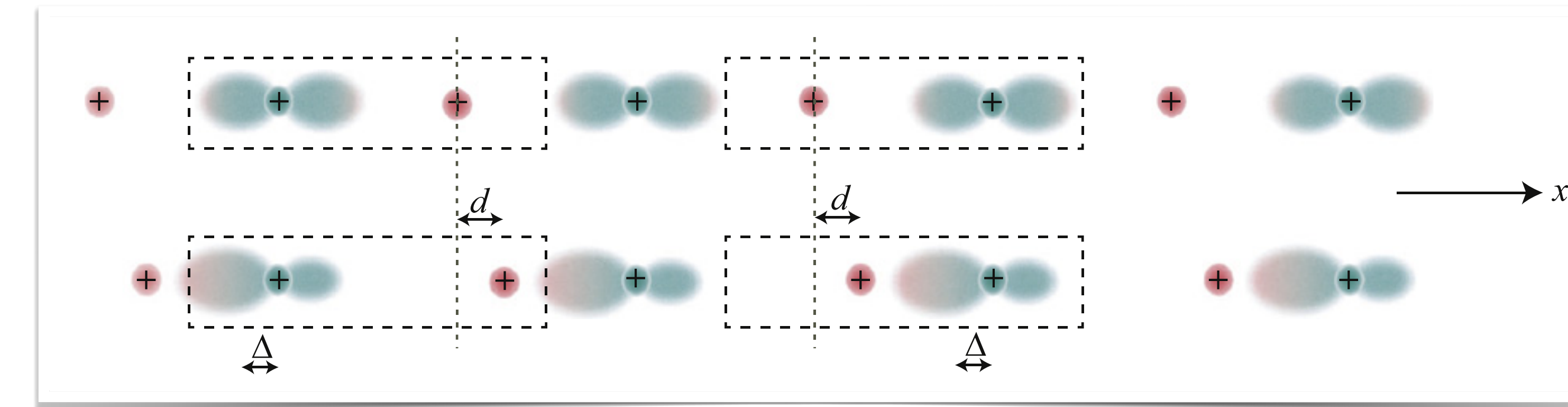


N.A. Spaldin, Journal of Solid State Chemistry 195, 2-10, (2012)





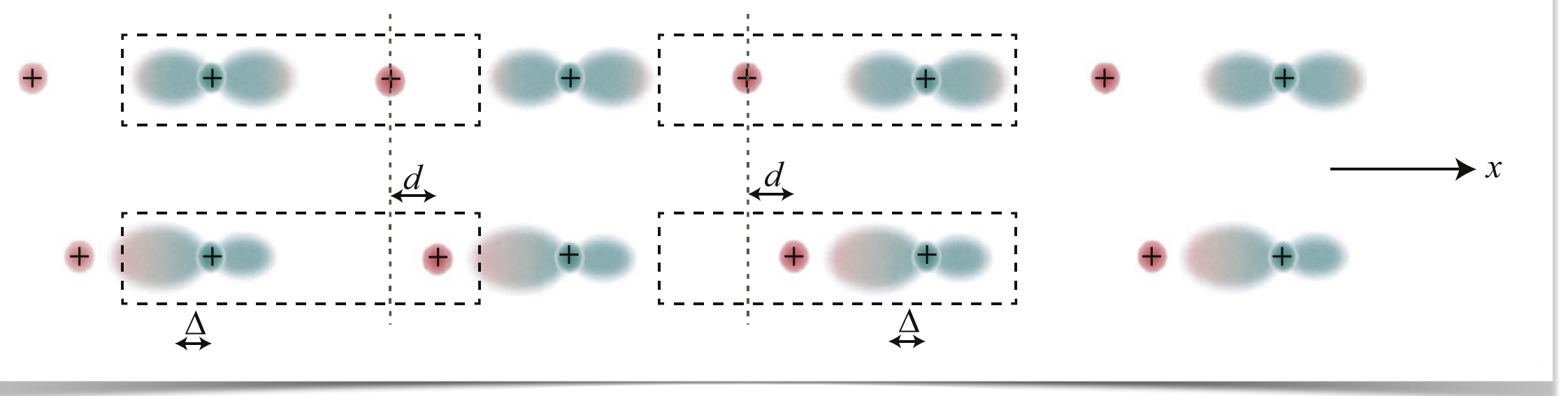
$$\begin{aligned} w_n(\mathbf{r}-\mathbf{R}) &= \frac{\Omega}{(2\pi)^3} \int_{BZ} d^3\mathbf{k} e^{-i\mathbf{k}\cdot\mathbf{R}} \Psi_{n\mathbf{k}}(\mathbf{r}) \\ &= \frac{\Omega}{(2\pi)^3} \int_{BZ} d^3\mathbf{k} e^{i\mathbf{k}\cdot(\mathbf{r}-\mathbf{R})} u_{n\mathbf{k}}(\mathbf{r}), \end{aligned}$$



N.A. Spaldin, Journal of Solid State Chemistry 195, 2-10, (2012)

$$\bar{\mathbf{r}}_n = \int w_n^*(\mathbf{r}) \mathbf{r} w_n(\mathbf{r}) d^3\mathbf{r}.$$

$$\mathbf{r} = -i(\partial/\partial\mathbf{k})$$



$$\bar{\mathbf{r}}_n = i \frac{\Omega}{(2\pi)^3} \int_{BZ} d^3\mathbf{k} e^{-i\mathbf{k}\cdot\mathbf{R}} \left\langle u_{n\mathbf{k}} \left| \frac{\partial u_{n\mathbf{k}}}{\partial \mathbf{k}} \right. \right\rangle.$$

$$p = \frac{1}{a} \left(\sum_i (q_i \chi_i)^{ions} + \sum_n^{occ} (q_n \bar{\mathbf{r}}_n)^{WFs} \right)$$

$$\begin{aligned} \delta p &= p^f - p^0 \\ &= \frac{1}{\Omega} \sum_i \left[q_i^f \mathbf{r}_i^f - q_i^0 \mathbf{r}_i^0 \right] \\ &\quad - \frac{2ie}{(2\pi)^3} \sum_n^{occ} \left[\int_{BZ} d^3\mathbf{k} e^{-i\mathbf{k}\cdot\mathbf{R}} \left\langle u_{n\mathbf{k}}^f \left| \frac{\partial u_{n\mathbf{k}}^f}{\partial \mathbf{k}} \right. \right\rangle - \left\langle u_{n\mathbf{k}}^0 \left| \frac{\partial u_{n\mathbf{k}}^0}{\partial \mathbf{k}} \right. \right\rangle \right], \end{aligned}$$

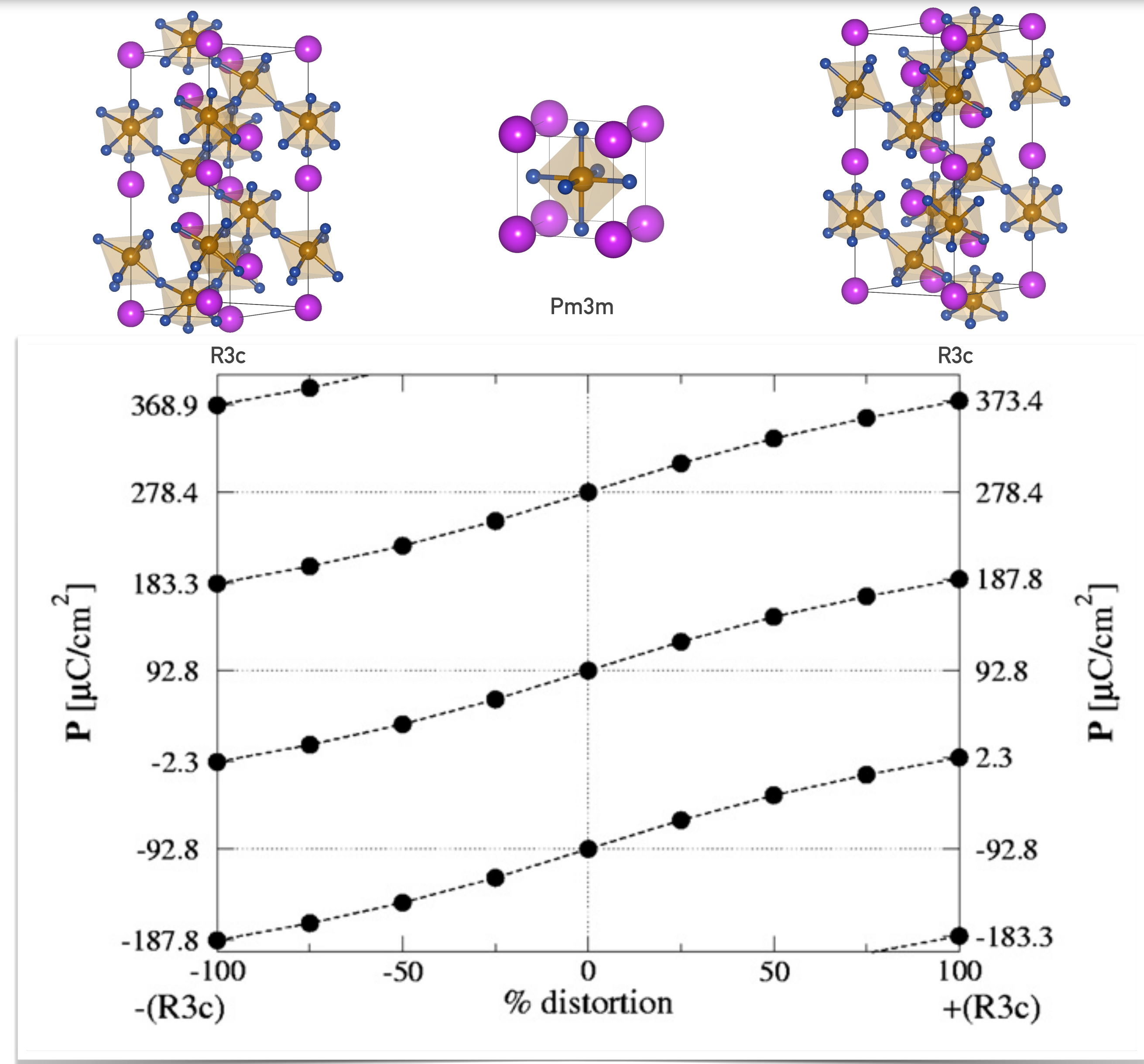
N. Marzari, D. Vanderbilt, Phys. Rev. B 56 (1997) 12847–12865.
 Gregory H. Wannier, Phys. Rev. 52, 191, (1937).

N.A. Spaldin, Journal of Solid State Chemistry 195, 2-10, (2012)

$$Z_{ij}^* = \frac{\Omega}{e} \frac{\delta P_i}{\delta d_j}.$$

	1^{st} -order	2^{nd} -order	
	$\partial/\partial\tau$	$\partial/\partial\eta$	$\partial/\partial\varepsilon$
$\partial/\partial\tau$	F	C	γ
$\partial/\partial\eta$	σ	γ	c^0
$\partial/\partial\varepsilon$	P	Z^*	e^0

A.C. Garcia-Castro, PhD - Thesis, (2016)



J.B. Neaton, C. Ederer, U.V. Waghmare, N.A. Spaldin, K.M. Rabe, Phys. Rev. B , 71, 014113 (2005).

Later and beyond...

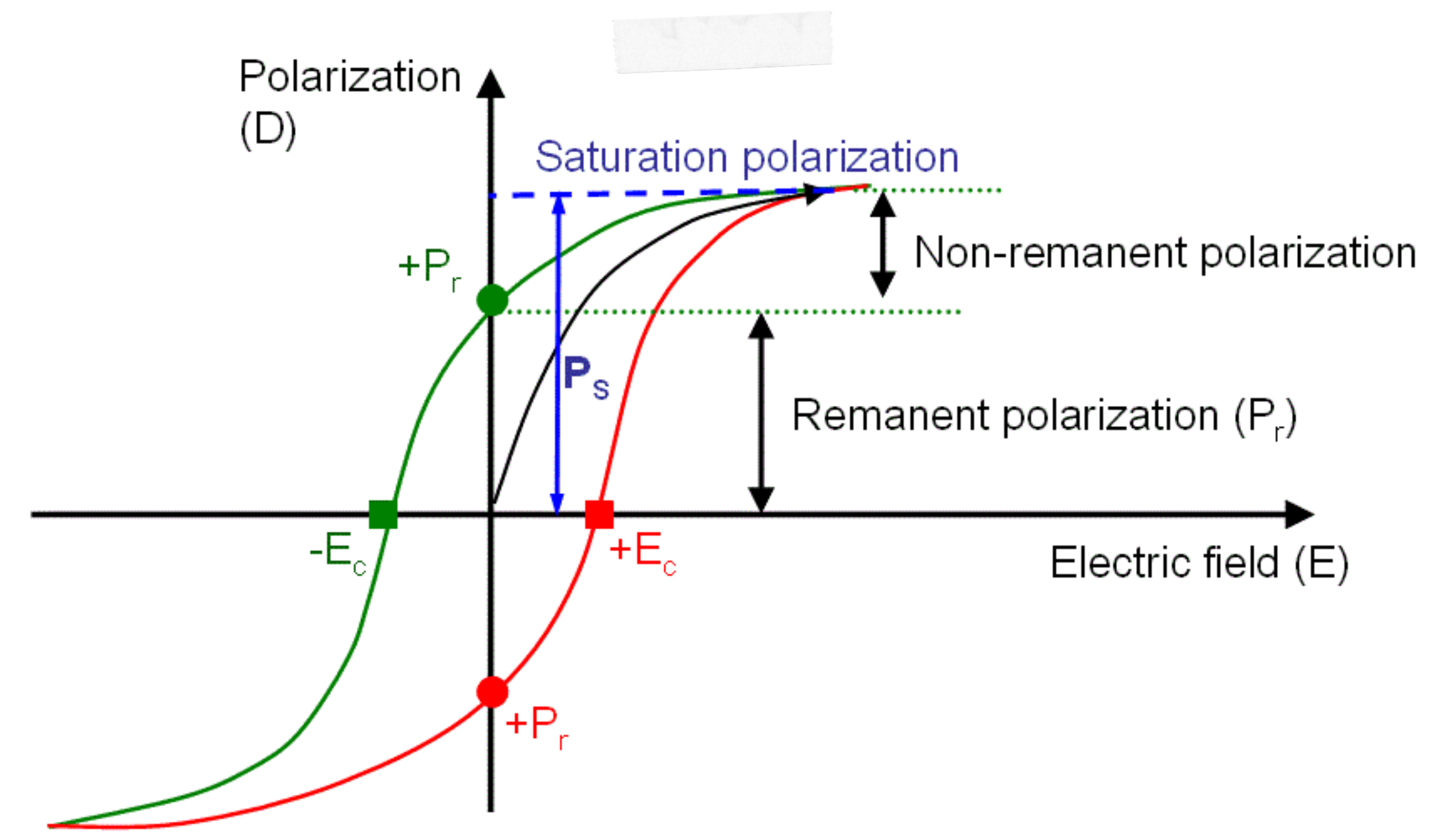
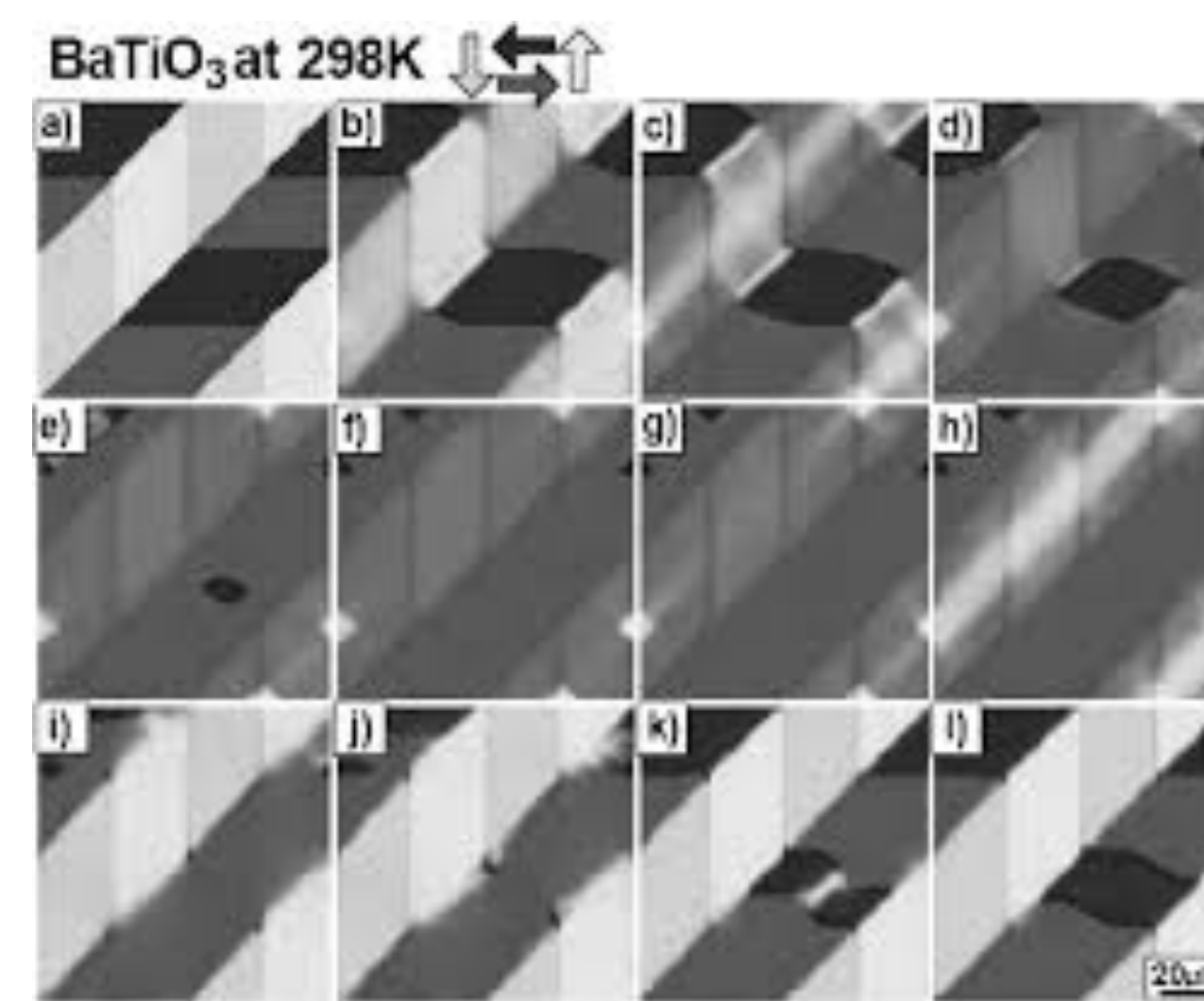
Multiferroics...

Ferroelectric-Rashba Materials...

Valleytronics...

Topological non-centrosymmetric systems...

Topological magnetic systems...



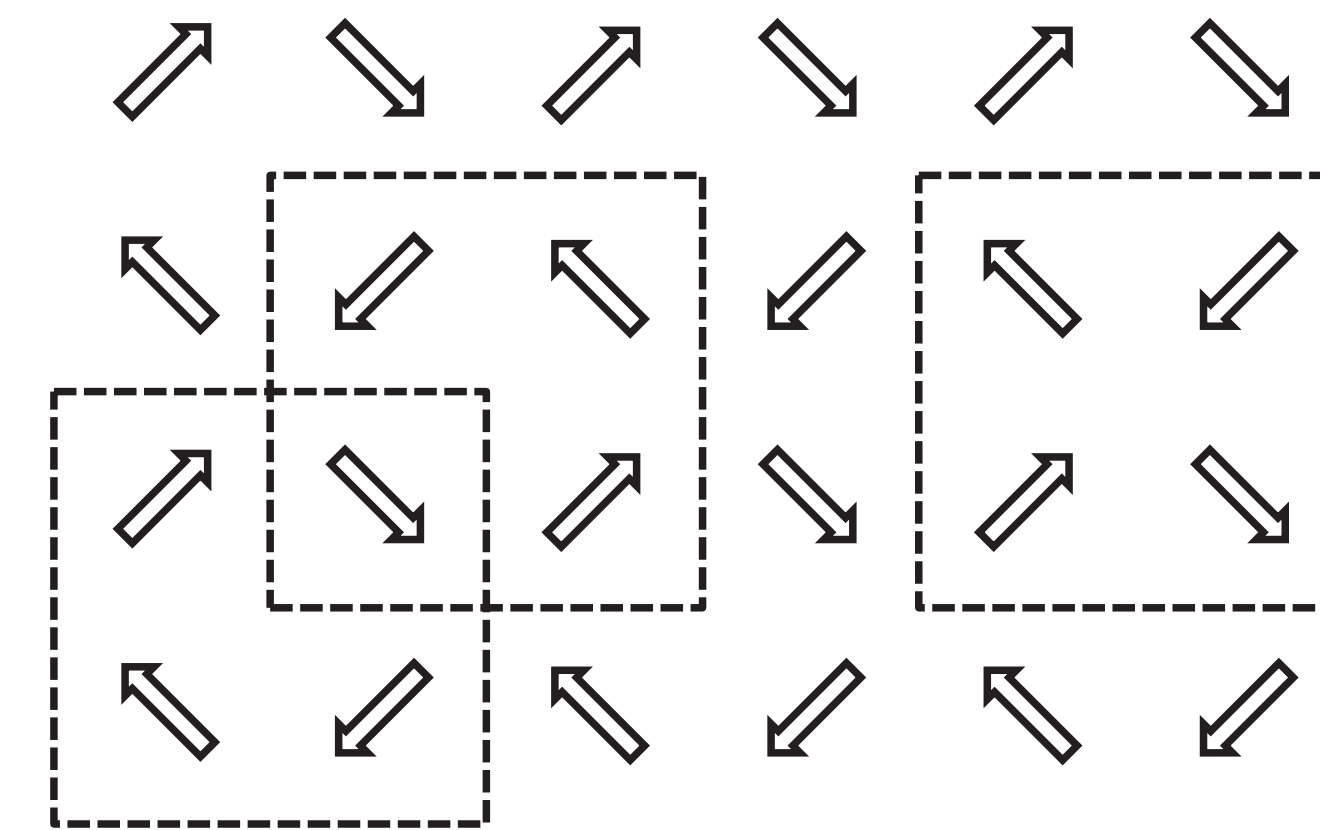
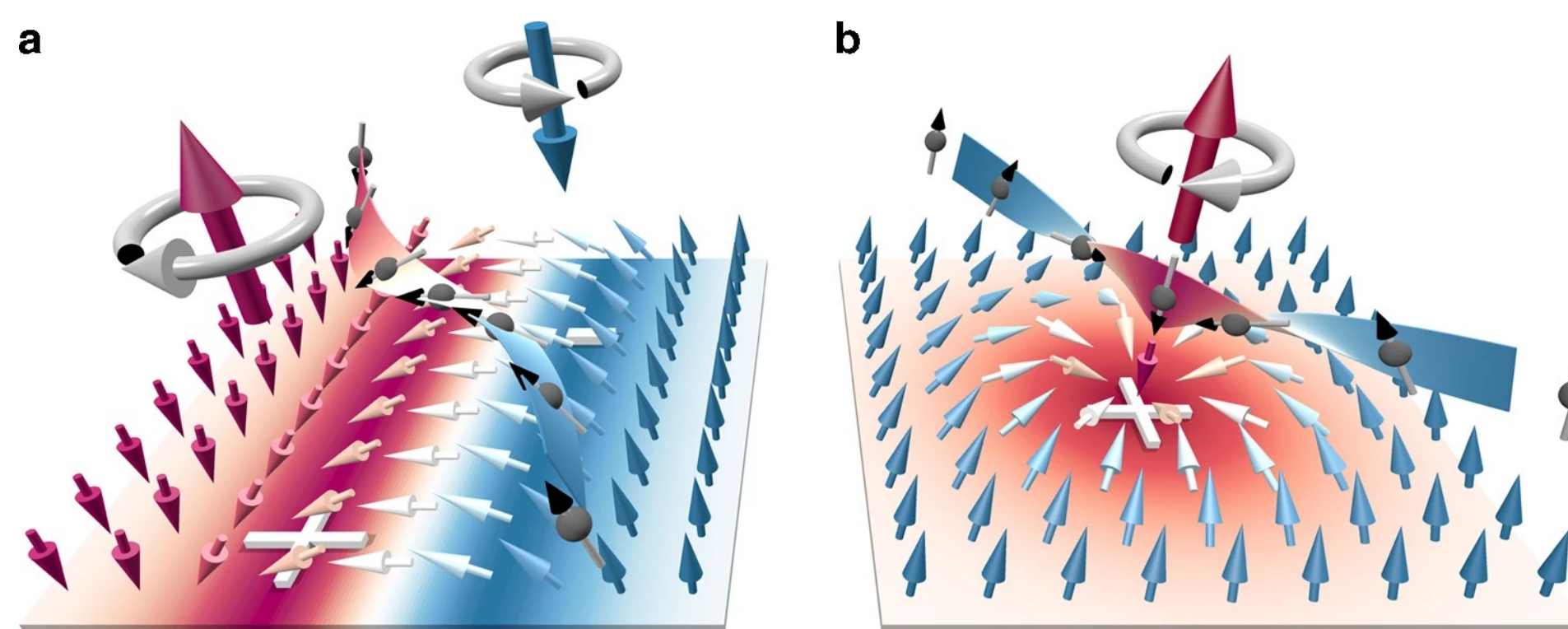


Figure 6.1 Model 2D crystal with broken time-reversal symmetry in which arrows indicate the local current flow pattern $\mathbf{j}(\mathbf{r})$. The three dashed squares indicate three different choices of unit cell boundaries that would give rise to very different definitions of orbital magnetization according to Eq. (6.2).



[Fabian R. Lux et al, Communications Physics, 1, 60 \(2018\)](#)

$$\begin{aligned}
 \mathbf{M} &= \frac{1}{V_{\text{cell}}} \sum_s \mathbf{m}_s \\
 \mathbf{m} &= \frac{-e}{2c} \sum_n^{\text{occ}} \langle \psi_n | \mathbf{r} \times \mathbf{v} | \psi_n \rangle \\
 \mathbf{M} &= \frac{e}{\hbar c} \frac{1}{(2\pi)^2} \sum_n \int_{\text{BZ}} \text{Im} \langle \partial_x u_{n\mathbf{k}} | H_{\mathbf{k}} + E_{n\mathbf{k}} - 2E_F | \partial_y u_{n\mathbf{k}} \rangle f_{n\mathbf{k}} d^2 k \\
 \mathbf{M} &= \frac{e}{2\hbar c} \frac{1}{(2\pi)^3} \sum_n \int_{\text{BZ}} \text{Im} \langle \nabla_{\mathbf{k}} u_{n\mathbf{k}} | \times (H_{\mathbf{k}} + E_{n\mathbf{k}} - 2E_F) | \nabla_{\mathbf{k}} u_{n\mathbf{k}} \rangle d^3 k.
 \end{aligned}$$

2D

Junren Shi, et al. Phys. Rev. Lett. 99, 197202

3D

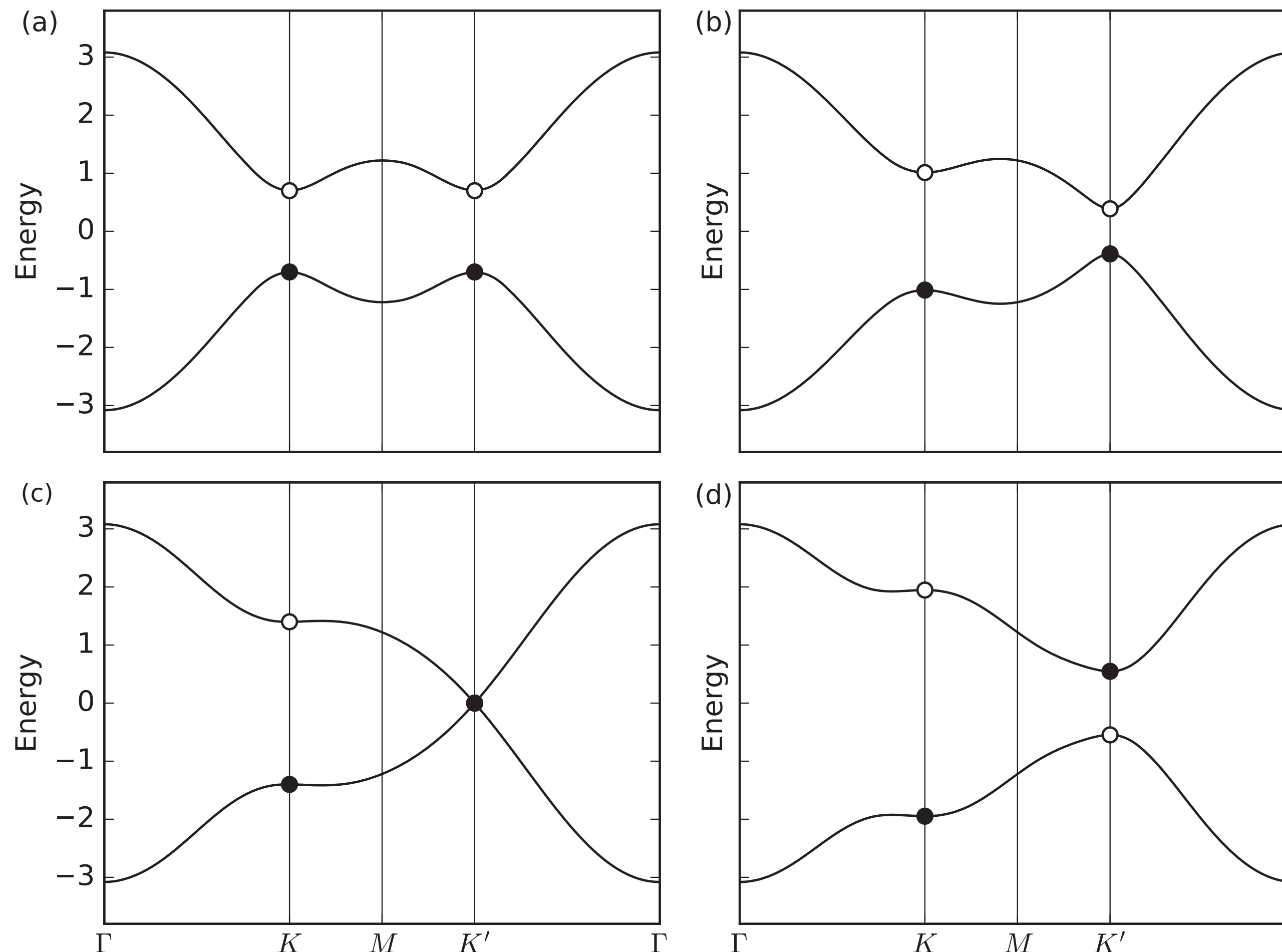


Figure 5.2 Band structures for the Haldane model of Eq. (5.1), with $\Delta = 0.7$, $t_1 = -1.0$, and (a) $t_2 = 0$; (b) $t_2 = -0.06$; (c) $t_2 = -0.1347$; (d) $t_2 = -0.24$. Filled (open) circles mark states of pure site-1 (site-2) character; band inversion at K' is evident in (d).

VOLUME 61, NUMBER 18 PHYSICAL REVIEW LETTERS 31 OCTOBER 1988

**Model for a Quantum Hall Effect without Landau Levels:
Condensed-Matter Realization of the “Parity Anomaly”**

F. D. M. Haldane
Department of Physics, University of California, San Diego, La Jolla, California 92093
 (Received 16 September 1987)

A two-dimensional condensed-matter lattice model is presented which exhibits a nonzero quantization of the Hall conductance σ^{xy} in the *absence* of an external magnetic field. Massless fermions *without spectral doubling* occur at critical values of the model parameters, and exhibit the so-called “parity anomaly” of (2+1)-dimensional field theories.

PACS numbers: 05.30.Fk, 11.30.Rd

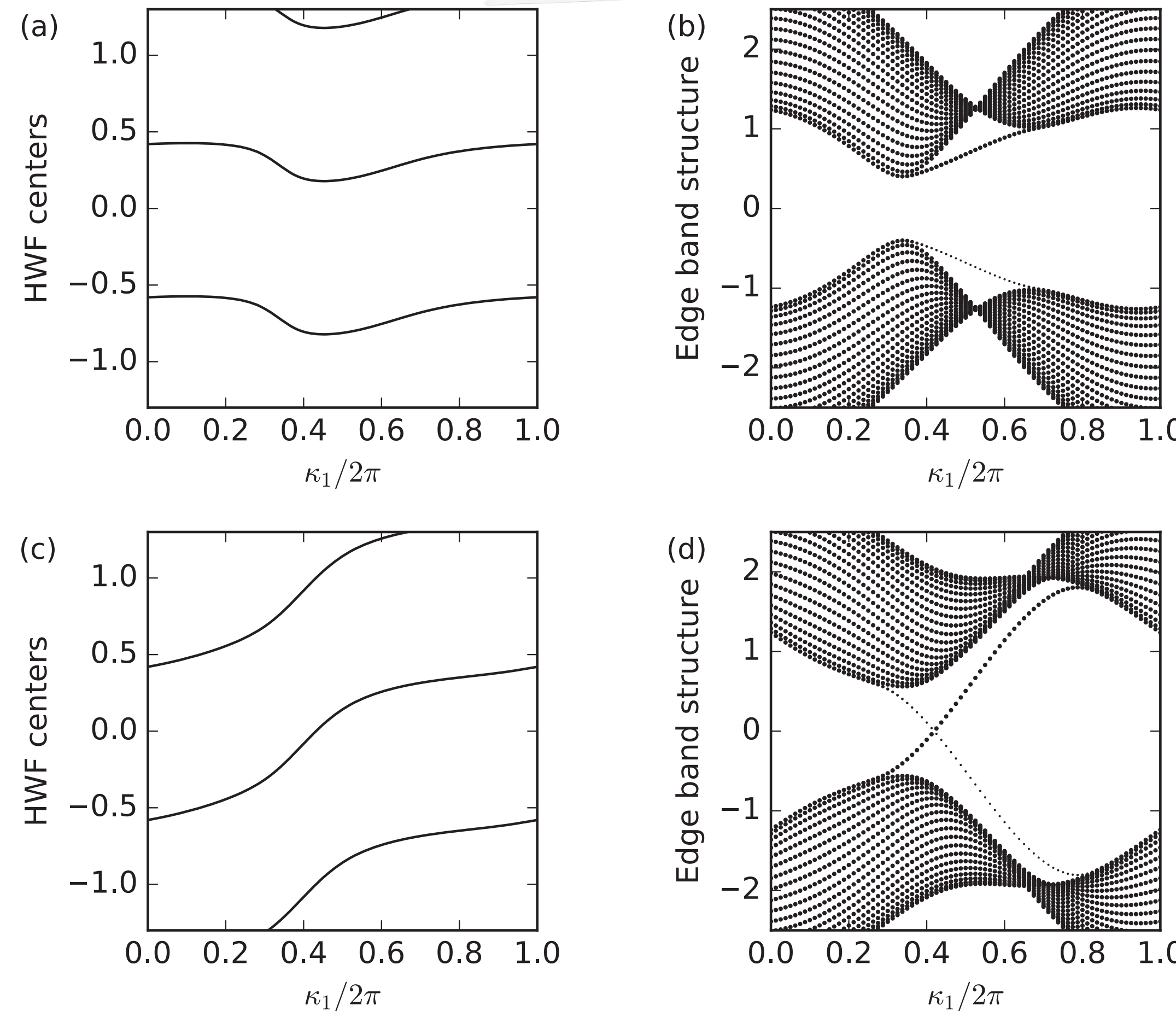


Figure 5.4 Flow of (a) hybrid Wannier centers, and (b) edge state energies on a ribbon cut from the Haldane model with $\Delta=0.7$ and $t_1=-1.0$ in the trivial phase, $t_2=-0.06$. (c-d) Same, but in the topological phase, $t_2=-0.24$. Surface states on the top and bottom edges of the ribbon are indicated by full and reduced intensity, respectively.

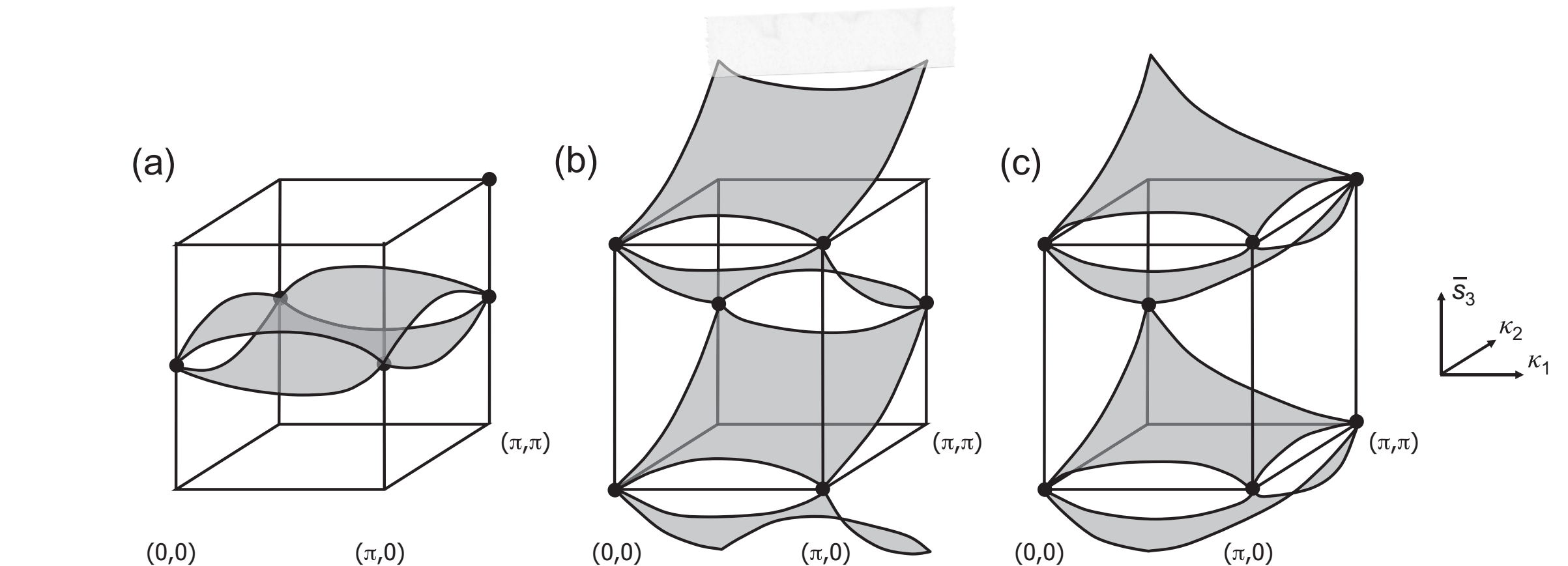


Figure 5.16 Sketches of possible flows of the hybrid Wannier center sheets $\bar{s}_3(\kappa_1, \kappa_2)$ versus in-plane wavevector for a TR-invariant insulator. One real-space repeat unit in the s_3 direction is shown. (a) Normal insulator with $\nu_1 = \nu'_1 = \nu_2 = \nu'_2 = 0$. (b) Weak TI with $\nu_1 = 1, \nu'_1 = 1, \nu_2 = 0, \nu'_2 = 0$. (c) Strong TI with $\nu_1 = 1, \nu'_1 = 0, \nu_2 = 0, \nu'_2 = 1$.

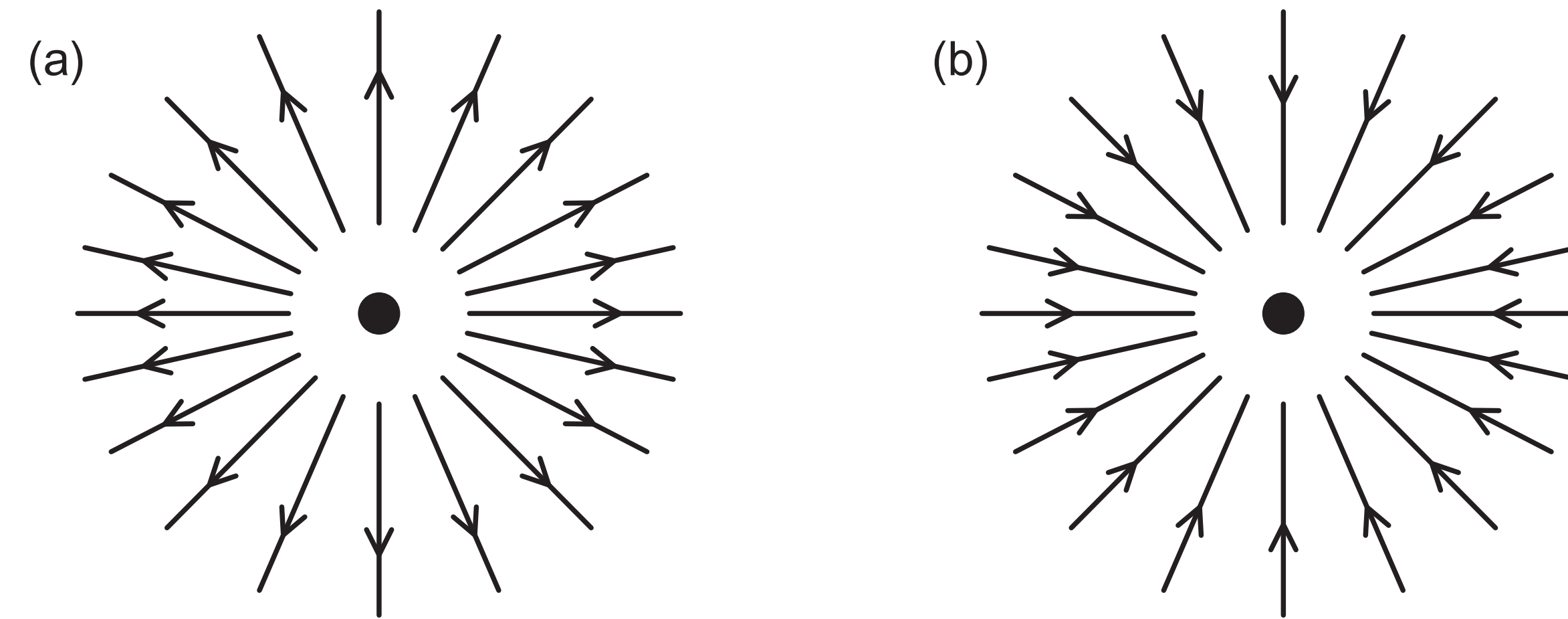


Figure 5.22 Sketch showing flux of Berry curvature of the lower-energy band emerging from or vanishing into the Weyl point at the center. (a) Negative chirality, $\chi = -1$. (b) Positive chirality, $\chi = +1$.

A band touching of the kind described by Eq. (5.32) is known as a *Weyl point* because of the resemblance of Eq. (5.32) to the famous Weyl Hamiltonian

$$H(\mathbf{p}) = \chi c \mathbf{p} \cdot \boldsymbol{\sigma} \quad (5.33)$$

$$\psi_n(\mathbf{r}) = \sum_j C_{nj} \varphi_j(\mathbf{r} - \boldsymbol{\tau}_j)$$

↓

$$H|\psi_n\rangle = E_n|\psi_n\rangle$$

↓

$$(H - E_n S) C_n = 0$$

Site energies and hoppings

$$H_{ij} = \langle \varphi_i | H | \varphi_j \rangle,$$

Overlaps

$$S_{ij} = \langle \varphi_i | \varphi_j \rangle,$$

↑

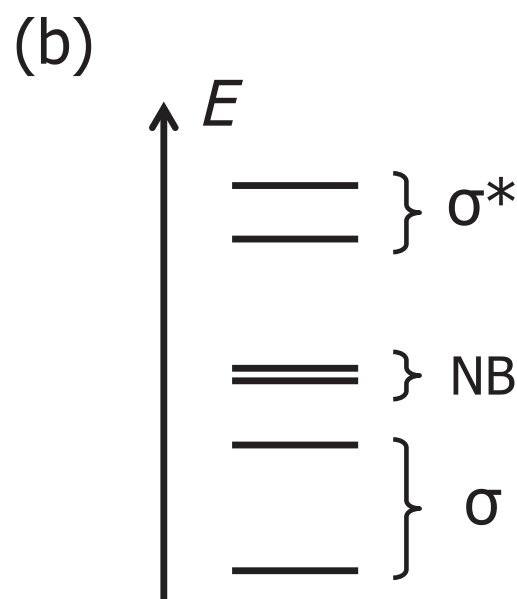
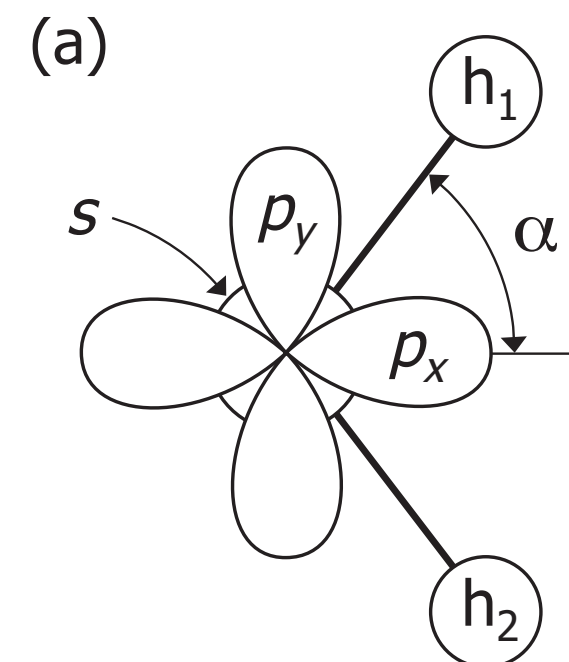


Figure 2.2 (a) Empirical tight-binding model for the water molecule. The oxygen p_z orbital, directed out of the plane, is not shown. (b) Eigenspectrum showing unoccupied antibonding (σ^*) orbitals and occupied nonbonding (NB) and bonding (σ) orbitals.

$$H_{\text{H}_2\text{O}} = \begin{pmatrix} E_s & 0 & 0 & 0 & t_s & t_s \\ 0 & E_p & 0 & 0 & t_p \cos \alpha & t_p \cos \alpha \\ 0 & 0 & E_p & 0 & t_p \sin \alpha & -t_p \sin \alpha \\ 0 & 0 & 0 & E_p & 0 & 0 \\ t_s & t_p \cos \alpha & t_p \sin \alpha & 0 & E_h & 0 \\ t_s & t_p \cos \alpha & -t_p \sin \alpha & 0 & 0 & E_h \end{pmatrix}$$

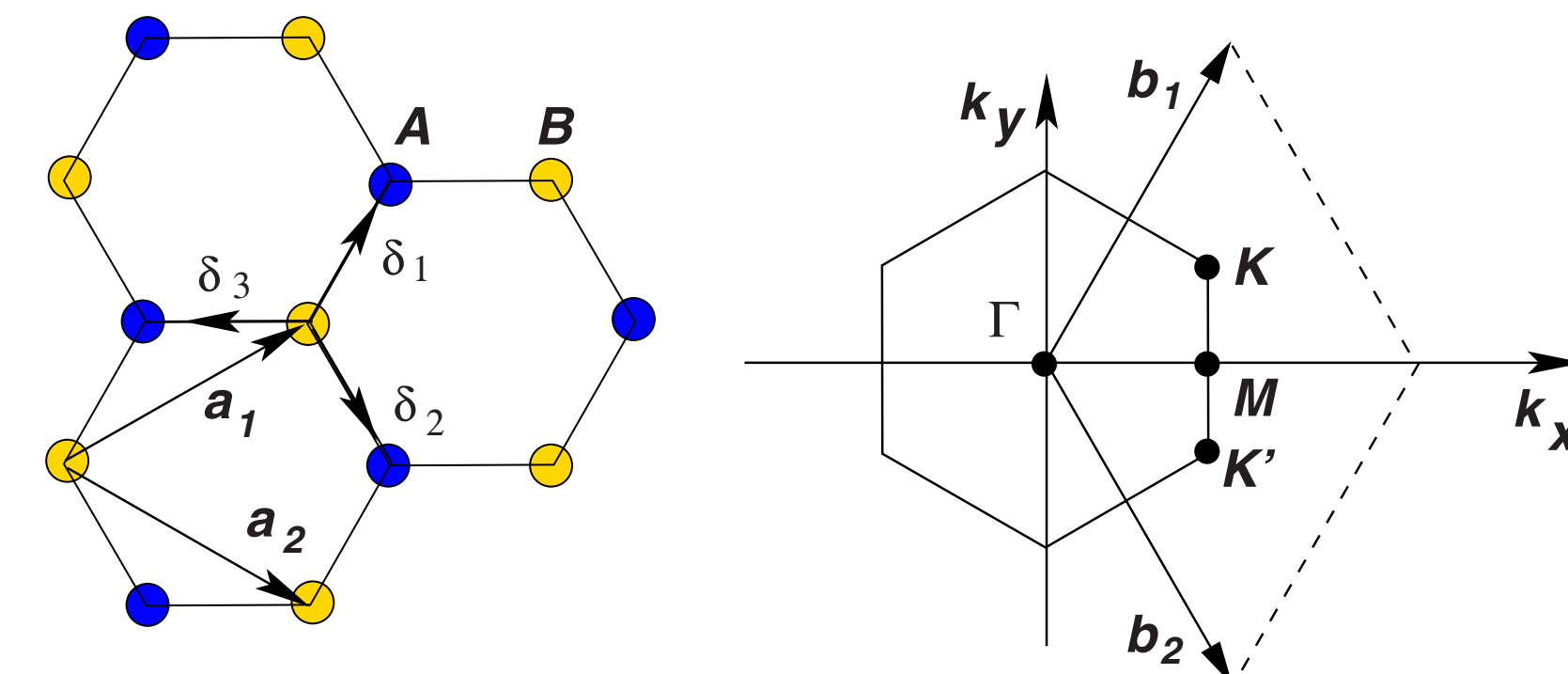


FIG. 2. (Color online) Honeycomb lattice and its Brillouin zone. Left: lattice structure of graphene, made out of two interpenetrating triangular lattices (\mathbf{a}_1 and \mathbf{a}_2 are the lattice unit vectors, and δ_i , $i=1,2,3$ are the nearest-neighbor vectors). Right: corresponding Brillouin zone. The Dirac cones are located at the K and K' points.

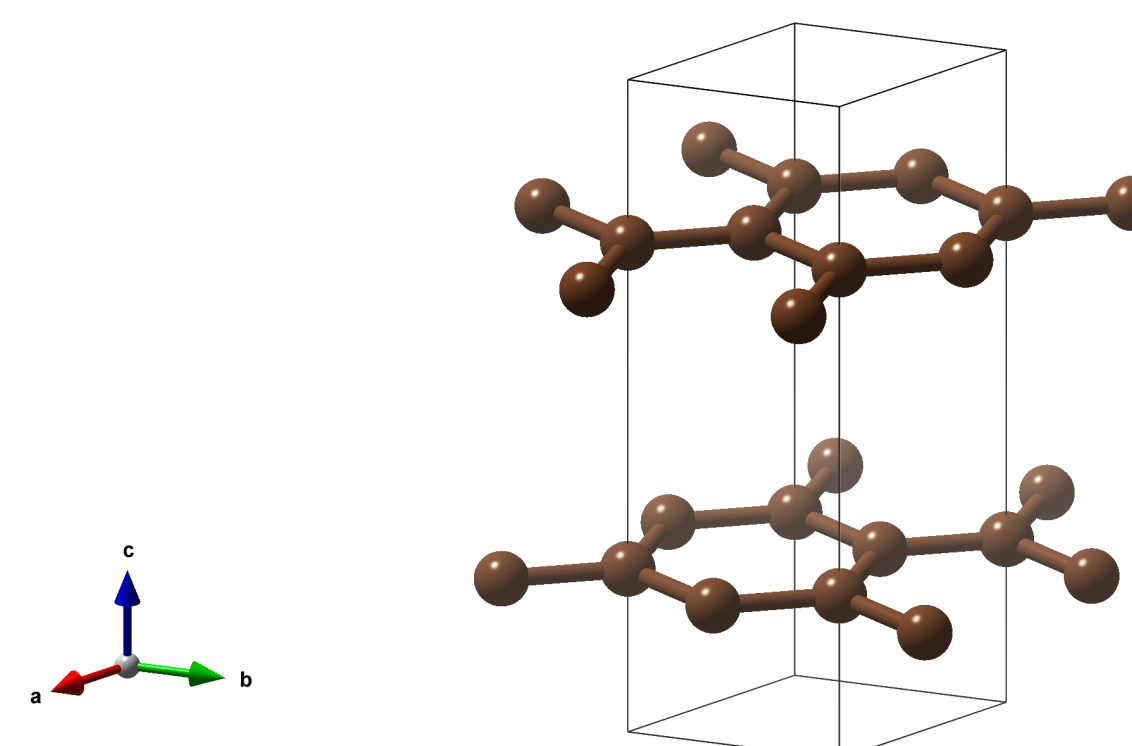


FIG. 3. (Color online) Electronic dispersion in the honeycomb lattice. Left: energy spectrum (in units of t) for finite values of t and t' , with $t=2.7$ eV and $t'=-0.2t$. Right: zoom in of the energy bands close to one of the Dirac points.

A. H. Castro Neto, et al., Rev. Med. Phys., 81, (2009).



The screenshot shows the PythTB 1.8.0 documentation page. The main title is "Python Tight Binding (PythTB)". A brief description states: "PythTB is a software package providing a Python implementation of the tight-binding approximation. It can be used to construct and solve tight-binding models of the electronic structure of systems of arbitrary dimensionality (crystals, slabs, ribbons, clusters, etc.), and is rich with features for computing Berry phases and related properties." Below this is a navigation menu with links: About, Installation, Examples, Formalism, Usage, and Resources. A "Quick search" input field with a "Go" button is also present. The "Quick installation" section contains instructions to type "pip install pythtb --upgrade" in the terminal. The "Quick example" section provides a simple example for defining a graphene tight-binding model and includes a link to more examples.

PythTB: <https://www.physics.rutgers.edu/pythtb/>

PythTB Formalism: [https://www.physics.rutgers.edu/pythtb/ downloads/e39c23ce476d399b268efa520e7a9091/pythtb-formalism.pdf](https://www.physics.rutgers.edu/pythtb/downloads/e39c23ce476d399b268efa520e7a9091/pythtb-formalism.pdf)

Obtain:

- Electronic Bands.*
- Berry phase, curvature and connection,*
- Explain your results and the model...!!!*

Gracias por su atención! Preguntas?
Comentarios?



Advancing
Innovation

Universidad
Industrial de
Santander

